



UNIVERSIDADE D
COIMBRA

Ana Margarida Pascoal Realinho

**IMPACT OF MATERNAL DIABETES ON
OFFSPRING RETINAL STRUCTURE AND
FUNCTION**

**Dissertação no âmbito do Mestrado em Engenharia Biomédica,
ramo de Instrumentação Biomédica, orientada pela Doutora
Filipa Isabel Cabaço Baptista e co-orientada pelo Doutor António
Francisco Ambrósio e apresentada à Faculdade de Ciências e
Tecnologia da Universidade de Coimbra.**

Setembro de 2022

Impact of maternal diabetes on offspring retinal structure and function

Ana Margarida Pascoal Realinho

Dissertação no âmbito do Mestrado em Engenharia Biomédica, ramo de Instrumentação Biomédica, orientada pela Doutora Filipa Isabel Cabaço Baptista e co-orientada pelo Doutor António Francisco Ambrósio e apresentada à Faculdade de Ciências e Tecnologia da Universidade de Coimbra.

University of Coimbra

2022

The experimental work described in the present thesis was performed at Retinal Dysfunction and Neuroinflammation Lab, Coimbra Institute for Clinical and Biomedical Research (iCBR), Faculty of Medicine, University of Coimbra.



This work was supported by Foundation for Science and Technology (PEst UIDB/04539/2020 and UIDP/04539/2020) and Centro 2020 Regional Operational Programme (CENTRO-01-0145-FEDER-000008: BrainHealth 2020).



“For the things we have to learn before we can do them, we learn by doing them.”

— Aristotle

ACKNOWLEDGMENTS/AGRADECIMENTOS

Este projeto de dissertação foi o encerrar do meu percurso académico, todo ele marcado por aventuras e novas experiências que culminam na pessoa e estudante que sou hoje, e na profissional que serei no futuro. Estarei eternamente grata pela sorte que tive em estar rodeada pelas pessoas certas neste ano decisivo. Sem elas, não teria chegado onde estou e com a felicidade que sinto ao olhar para o caminho que percorri. Gostaria, por isso, de agradecer:

À minha orientadora, Filipa Baptista, por me ensinar muito do que sei hoje. Por toda a tua paciência ao estares presente quando eu precisava muito de apoio e por me deixares ir a pouco e pouco quando sentiste que era capaz. Tive muita sorte em ter uma orientadora como tu, sem ti não teria conseguido nem metade. Obrigada por me aceites neste projeto, por teres sido uma peça essencial na minha integração no grupo e por acreditares em mim quando eu própria não acreditava. Deixaste-me com o bichinho da investigação, pelo amor e dedicação que colocas em tudo o que fazes e o entusiasmo que me foste transmitindo. E é tão mais fácil trabalhar quando gostamos do que fazemos...

Ao Doutor Francisco Ambrósio, o meu co-orientador e líder do grupo, pelas palavras de incentivo ao longo do processo, pelo olhar atento e crítico que dedicou ao meu trabalho e pelas questões que foi levantando e que me fizeram pensar mais além. Agradeço-lhe também por se ter mostrado sempre uma pessoa acessível e pela forma como me incluiu a mim e aos restantes alunos de mestrado nas atividades do grupo, nomeadamente o piquenique, ajudando a quebrar barreiras e a unir as pessoas.

À Doutora Raquel Boia, por ter acompanhado este trabalho de perto, pelo rigor, honestidade e prontidão a ajudar sempre necessário. Obrigada pelos conselhos, por estares presente nos momentos de discussão e pela tua enorme contribuição nos ERGs e OCTs que foi essencial neste projeto. Aprendi muito contigo!

À Catarina Neves, por me convidares a aprender contigo nas tuas disseções do cérebro! Foi o meu primeiro contacto com os animais e a tua paciência e descontração foram essenciais. Obrigada pelas dicas que me foste dando no laboratório e no geral pelo à vontade e boa disposição.

A todos os elementos do Retinal Dysfunction and Neuroinflammation Lab, por me receberem como parte da vossa família, nas vossas tradições, rotinas e responsabilidades. Senti-me verdadeiramente inserida numa equipa de excelentes profissionais que tanto me ajudaram a crescer pessoal e profissionalmente, dentro e fora do laboratório. Fartei-me de aprender convosco! Um obrigada gigante pela vossa paciência a responder a todas (e muitas) perguntas que tive, pelas vossas sugestões quando viam que precisava de melhorar, pela companhia no dia-a-dia e por tornarem as horas passadas no laboratório muito fáceis de passar.

Ao Hugo e ao José, os meus colegas de dissertação, pelas horas de almoço de discussão, desabafos, partilha de experiências e amena cavaqueira no geral! Obrigada por responderem às minhas perguntas mais “estúpidas” e por todas as dicas técnicas, principalmente por parte do Hugo que foi praticamente um tutor de prática laboratorial. Foi giro trabalhar convosco!

À Marina e ao João, companheiros na Dinamarca, por me ajudarem a manter um equilíbrio saudável entre a vida de ERASMUS e as horas de pesquisa e leitura na biblioteca da CBS. Foi uma experiência que levarei para a vida.

Ao meu pessoal de Coimbra, Alexandra, António, Baltazar, Cortez, Diogo, Dora, Doze, Felamino, Mandinho, Moreira, Pedro, Pipa e Zé que já são quase família (reparem que tive de vos pôr por ordem alfabética para garantir que não falhava ninguém no meio de tanta gente) por ouvirem os meus desabafos e acompanharem as minhas conquistas em assuntos que provavelmente não vos dizem grande coisa. Obrigada pelos momentos de produtividade forçada na biblioteca de mecânica, por me desencaminharem de vez em quando em jantaras ou idas ocasionais à Praia da Tocha quando precisava de descontrair e de uma forma geral por fazerem parte da minha vida. Sois lindos!

Ao BEST, a organização que me acolheu nos últimos 4 anos e a todos os que se cruzaram comigo no meu percurso lá. Cresci muito nesta casa a nível pessoal, não sou seguramente a mesma pessoa que um dia entrou timidamente no 1º recrutamento. Se hoje estou aqui, é porque o BEST me deu muitas das ferramentas necessárias. Em especial, agradeço à Nena, Hugo, Inês, MarySal e Carvalhão que acompanharam mais de perto a minha jornada!

Aos amigos da terrinha, Ana, Inês, Mariana, Miguel e Rita. Os de sempre e que estarão lá até sermos velhinhos, porque independentemente de estarmos mais longe ou mais perto, sei que estão lá para o que der e vier. Obrigada pelo apoio que me têm dado e por acreditarem tanto em mim e nas minhas capacidades. Adoro-vos mil!

Ao meu gatinho Nolan (Tico para os amigos), o gato da Cidade, por ser tão fofinho em tudo o que faz que só de o observar fico mais calma. Sem o saber, e sem ter grande escolha, coitado, foi um grande apoio emocional para mim. Quem diz que os gatos são frios e não querem saber dos donos claramente não conhece o Nolan.

Por último, aos meus pais e mano, pelo apoio incondicional e confiança que depositam em mim. As melhores qualidades que tenho devo ao ambiente familiar em casa que me proporcionaram desde sempre, com as nossas discussões acesas à hora da refeição sobre todos os assuntos possíveis, os momentos de desabafo, os sermões, as viagens e atividades em conjunto... foram sem dúvida um pilar este ano, tal como têm sido em todos os outros. Obrigada por acreditarem no meu sucesso, devo-vos o mundo.

Como John Donne diria, “*No man is an Island*”. Um obrigada a todos os que, de uma maneira ou de outra, contribuíram para que chegasse aqui.

TABLE OF CONTENTS

LIST OF FIGURES	xv
LIST OF TABLES.....	xvii
ABBREVIATIONS LIST	xix
RESUMO	xxi
ABSTRACT.....	xxi
GRAPHICAL ABSTRACT	xxv
SCIENTIFIC COMMUNICATIONS.....	1
Chapter 1: Introduction	3
1.1. Anatomy of the retina.....	5
1.2. Retina development.....	7
1.2.1. Overview	7
1.2.2. Synaptogenesis.....	8
1.2.3. Synaptic transmission	9
1.2.4. Role of microglia.....	11
1.3. Diabetes mellitus	13
1.3.1. Diabetes in pregnancy.....	13
1.3.2. Impact of maternal diabetes on offspring CNS	14
1.3.3. Impact on the developing retina	15
1.4. Aims.....	17
Chapter 2: Methods	19
2.1. Ethics statement	21
2.2. Animals.....	21
2.3. Weight and glycemia.....	22
2.4. Eye opening.....	22
2.5. Electroretinogram	22
2.5.1. ERG recordings.....	24
2.5.2. ERG analysis	24
2.6. Optical coherence tomography	25
2.6.1. OCT recordings.....	26
2.6.2. OCT analysis.....	26
2.7. Western Blot	26

2.7.1.	Sample collection	26
2.7.2.	Total extract preparation.....	26
2.7.3.	BCA protein quantification	26
2.7.4.	SDS-PAGE western blot.....	27
2.8.	Immunohistochemistry	28
2.8.1.	Sample collection and embedding.....	28
2.8.2.	Cryosections and wholemounts tissue preparation	29
2.8.3.	Sectioning using a cryostat.....	29
2.8.4.	Immunohistochemistry of retinal cryosections	29
2.8.5.	Fluorescence immunostaining of wholemounts	30
2.8.6.	Image acquisition and analysis.....	31
2.9.	Microglia branched structure analysis and sholl analysis	31
2.10.	Statistical analysis.....	32
Chapter 3:	Results.....	33
3.1.1.	Metabolic characterization of the dams and litter size	35
3.1.2.	Effect of maternal diabetes on offspring's bodyweight, glycemia and eye-opening day	36
3.2.	Impact of maternal diabetes on offspring retina development at early infancy	38
3.2.1.	Maternal diabetes does not induce changes in retinal synaptic and neuronal protein levels in male and female offspring at early infancy.....	38
3.2.2.	Maternal diabetes does not induce changes in the number of RGCs in male and female offspring at early infancy	40
3.2.3.	Impact of maternal diabetes on microglia number, morphology, and CX3CR1 protein levels at early infancy	41
3.3.	Impact of maternal diabetes on offspring retina at late infancy	43
3.3.1.	Diabetes during pregnancy induces changes in retinal structure.....	43
3.3.2.	Diabetes during pregnancy induces changes in offspring retinal function	45
3.3.3.	Impact of maternal diabetes on offspring retinal synapses and neurons at late infancy.....	47
3.3.4.	Maternal diabetes does not induce changes in the number of RGCs in male and female offspring at late infancy	49
3.3.5.	Impact of maternal diabetes on microglia number, morphology, and CX3CR1 protein levels at late infancy	50

Chapter 4: Discussion	55
4. Discussion	57
Chapter 5: Conclusions	63
5. Conclusions	65
References	67

LIST OF FIGURES

Figure 1: Anatomy of the eye	5
Figure 2: Schematic figure of the anatomy of the retina.	6
Figure 3: Time course of mice retinal development.....	7
Figure 4: Cellular structure of the retina, showing the ON and OFF pathways	10
Figure 5: Distribution of microglia in the developing rodent retina and schematic representations of amoeboid versus ramified morphology.....	12
Figure 6: Schematic figure of the general timeline	21
Figure 7: Dark adapted (scotopic) ERG showing the a-wave, b-wave and OPs.....	23
Figure 8: Light adapted (photopic) ERG showing the b-wave and OPs.....	23
Figure 9: Typical OCT image of a P21 rat analysed with Insight along with corresponding layers.....	25
Figure 10: Schematic figure of a microglia cell analyzed with Neurolucida software	31
Figure 11: Dam bodyweight and glycemia at the beginning and end of gestation and number of pups per litter	35
Figure 12: Effects of maternal diabetes in male and female offspring bodyweight and glycemia levels at early (P7) and late infancy (P21)	37
Figure 13: Diabetes during pregnancy leads to a delay in offspring eye opening, while insulin administration expedites it.....	38
Figure 14: Maternal diabetes does not induce changes retinal synaptic and neuronal protein levels in male and female offspring at P7.....	39
Figure 15: Maternal diabetes does not induce changes in the number of RGCs in male and female offspring at P7.....	40
Figure 16: Diabetes during pregnancy does not impact microglia number, morphology and fractalkine receptor levels in the retina at early infancy.....	42
Figure 17: Diabetes during pregnancy induces changes in retina morphology	44
Figure 18: Diabetes during pregnancy induces changes in retinal function	46
Figure 19: Maternal diabetes does not induce changes in male and female offspring synaptic and neuronal protein levels in the retina at P21	48
Figure 20: Maternal diabetes does not induce changes in male and female offspring number of RGCs at P21.....	49
Figure 21: Maternal diabetes induces changes in arrestin levels in females.....	50
Figure 22: Diabetes during pregnancy does not induce changes in microglia number, morphology and fractalkine receptor levels in late infancy	52

LIST OF TABLES

Table 1: Primary antibodies used for Western Blot.	28
Table 2: Secondary antibodies used for Western Blot.	28
Table 3: Primary antibodies used for cryostat slices immunostaining.	30
Table 4: Secondary antibodies used for cryostat slices immunostaining.	30
Table 5: Primary antibodies used for wholemounts immunostaining.	30
Table 6: Secondary antibodies used for wholemounts immunostaining.	30

ABBREVIATIONS LIST

A

ANOVA – One-way analysis of variance
ARVO – Association for Research in Vision and Ophthalmology

B

BCA – Bicinchoninic acid
BSA – Bovine serum albumin

C

CNS – Central nervous system
CX3CR1 – Fractalkine receptor

E

E – Embryonic day
ECF – Enhanced chemifluorescence
ECL – Enhanced chemiluminescence

G

G – Gestational day
GCL – Ganglion cell layer
GDM – Gestational diabetes
GFAP – Glial fibrillary acidic protein

I

IHC – Immunohistochemistry
INL – Inner nuclear layer
IP – Intraperitoneal
IPL – Inner plexiform layer
IS/OS – Inner/outer segment layer

N

NCL – Neuroblastic cell layer
NeuN – Neuronal nuclear protein
NFL – Nerve fiber layer

nSTR – Negative scotopic threshold response

O

OCT – Optical coherence tomography
ONL – Outer nuclear layer
OPL – Outer Plexiform layer
OPs – Oscillatory potentials

P

P – Postnatal day
PBS – Phosphate buffered saline
PFA – Paraformaldehyde
PSD – Postsynaptic density
pSTR – Positive scotopic threshold response

R

RGCs – Retinal Ganglion cells
RPE – Retinal Pigment epithelium

S

SDS – Sodium dodecyl sulfate
SEM – Standard error of the mean
STR – Scotopic threshold response
STZ – Streptozotocin

T

T1D – Type 1 diabetes
T2D – Type 2 diabetes

V

VGLuT – Vesicular glutamate transporter

RESUMO

A diabetes durante a gravidez está associada a um risco aumentado para distúrbios do neurodesenvolvimento na descendência, com um impacto negativo a nível do cérebro, e dando origem a efeitos adversos de curto e longo prazo. A retina, que faz parte do sistema nervoso central (CNS) e é considerada uma extensão do cérebro, pode também ser vulnerável à diabetes durante a gravidez, desconhecendo-se os seus efeitos em termos do impacto no desenvolvimento, estrutura e função da retina.

Com este trabalho, pretendeu-se avaliar o impacto da diabetes materna no desenvolvimento, estrutura e função da retina, com foco no período da infância. Além disso, como a diabetes materna já foi descrita como tendo efeitos dependentes do sexo no cérebro da descendência, teve-se como objetivo também esclarecer se a retina de machos e fêmeas tem uma diferente suscetibilidade à hiperglicémia durante o desenvolvimento. Ao mesmo tempo, pretendeu-se analisar se a administração de insulina à mãe, tratamento padrão para a diabetes, pode prevenir alterações na retina da descendência induzida pela diabetes materna.

O modelo animal de diabetes tipo 1 pré-gestacional (T1D) foi obtido através de uma única injeção intraperitoneal (IP) de estreptozotocina (STZ: 45 mg/kg) em ratos fêmea em jejum. Três dias após a injeção de STZ foi introduzido subcutaneamente um implante de insulina (~1 U/dia; Linplant®) a um subgrupo de fêmeas diabéticas. Os níveis de glicémia das fêmeas foram monitorizados para confirmar a presença de diabetes durante o período de gestação e para confirmar a normoglicémia em mães com implante de insulina e controlos. O peso das mães também foi monitorizado antes e durante o período de gestação. Após o nascimento, foi contado o número de crias por ninhada e os descendentes foram monitorizados durante os dias seguintes para avaliar o dia de abertura dos olhos. O peso e a glicémia dos machos e fêmeas descendentes das mães controlo (CTRL), diabéticas (STZ) e diabéticas tratadas com insulina (STZ+INS) foram avaliados no dia pós-natal (P)7 e 21. A estrutura e função da retina foram avaliadas *in vivo* por meio de tomografia de coerência ótica (OCT) e eletrorretinograma, respetivamente, a P21. Amostras de tecido retiniano foram utilizadas para análise molecular e celular por Western Blot e imunohistoquímica (IHC), em ambos os períodos da infância em estudo.

Os valores de glicémia foram semelhantes nos descendentes de mães diabéticas e controlos a P7 e P21. No entanto, os descendentes de mães diabéticas apresentaram peso inferior durante o período da infância, sendo o tratamento da mãe com insulina capaz de prevenir totalmente esta alteração a P7, mas apenas parcialmente a P21. A diabetes materna induziu também um atraso no dia de abertura dos olhos da descendência quando comparado com os controlos. Curiosamente, o tratamento das mães diabéticas com insulina antecipou a abertura dos olhos dos descendentes comparativamente aos controlos, sugerindo uma maturação precoce.

A nível molecular, o conteúdo de proteínas sinápticas na retina não foi alterado nos descendentes de mães diabéticas quando comparados com os descendentes de mães controlo, tanto a P7 como a P21. No entanto, nas descendentes fêmea de mães diabéticas houve tendência para uma redução dos níveis de sinapsina a P7. O número de células ganglionares da retina (RGCs) não foi afetado pela diabetes materna e o número e morfologia das células da microglia não sofreram alterações em ambos os períodos.

Relativamente à estrutura da retina, a diabetes materna induziu uma redução na espessura da camada dos segmentos internos e externos dos fotorreceptores tanto em descendentes machos como em fêmeas, e uma redução na espessura da camada de fibras nervosas (NFL), camada das células ganglionares (GCL) e camada plexiforme interna (IPL), a P21, mas apenas nas fêmeas. Este efeito não foi associado a perda de células ganglionares e foi prevenido pela administração de insulina às mães diabéticas. Em relação à função retiniana, a diabetes materna induziu uma diminuição da amplitude da 1ª harmónica do *flicker* e da onda-b escotópica em descendentes do sexo masculino, indicando disfunção dos cones e células bipolares, respetivamente, tendo o tratamento com insulina prevenido estas alterações. As fêmeas descendentes de mães diabéticas parecem ser resilientes a alterações na função neuronal da retina. No entanto, os níveis da proteína arrestina na retina encontram-se diminuídos, um efeito prevenido pela administração de insulina. Não se observaram alterações nos níveis de arrestina em descendentes do sexo masculino.

Resumindo, a exposição a hiperglicémia durante a gravidez atrasou o dia de abertura dos olhos da descendência, sugerindo um impacto no desenvolvimento. Também afetou negativamente a retina da descendência, induzindo uma redução da espessura de várias camadas retinianas, com impacto evidente na função de células bipolares e fotorreceptores em machos, e uma redução nos níveis de arrestina em fêmeas. Os resultados mostram uma elevada suscetibilidade dos fotorreceptores à hiperglicémia, sendo estes neurónios particularmente vulneráveis à diabetes materna. A administração de insulina preveniu essas alterações.

Este trabalho permitiu aumentar o conhecimento acerca do impacto da diabetes materna no desenvolvimento da retina e pode inspirar trabalhos futuros na clarificação dos mecanismos subjacentes às alterações observadas. O trabalho destaca ainda a importância de avaliar a retina de crianças expostas à diabetes materna, particularmente na infância, mas também ao longo da vida, enfatizando a relevância da terapia com insulina, ao mesmo tempo em que chama a atenção para a importância de considerar as especificidades de cada sexo em estudos pré-clínicos.

Palavras-chave: Diabetes materna, Retina, Neurodesenvolvimento, Sinapse, Microglia, Diferenças de sexo

ABSTRACT

Diabetes during pregnancy is associated with increased risk of neurodevelopmental disorders in the offspring, negatively impacting the offspring brain and giving rise to short- and long-term adverse effects. The retina, which is part of the central nervous system (CNS) and is considered an extension of the brain, may also be vulnerable to diabetes during pregnancy, with unknown effects in its development, structure, and function.

With this work, we intended to evaluate the impact of maternal diabetes on retina development, structure and function, focusing on infancy period. Additionally, since maternal diabetes was already described to have a sex-specific impact in the offspring's brain, we aimed to clarify if males and females' retinas have a different vulnerability to hyperglycemia during development. At the same time, we aim to address if dam treatment with insulin, the gold standard therapy for diabetes, can prevent any offspring retinal alteration induced by maternal diabetes.

Pre-gestational type 1 diabetes (T1D) animal model was achieved by a single intraperitoneal (IP) injection of streptozotocin (STZ: 45 mg/kg) in fasting female rats. Three days after STZ injection, a subset of diabetic females received an insulin implant (~1 U/day; Linplant®) subcutaneously. Dams' glycemia was monitored to confirm diabetes during gestation period and to confirm normoglycemia in dams with insulin implant and controls. Weight was also monitored before gestation and during gestation period. After birth of the offspring, the number of pups per litter was counted and offspring were closely monitored during the following days to evaluate eye opening day. Male and female offspring weight and glycemia of control (CTRL), diabetic (STZ) and diabetic treated with insulin (STZ+INS) dams were evaluated at postnatal day (P)7 and 21. Retina structure and function were evaluated *in vivo* by optical coherence tomography (OCT) and electroretinogram, respectively, at P21. Retinal tissue samples were used for molecular and cellular analysis by Western Blot and immunohistochemistry (IHC), in both time points.

Glycemia values were similar between diabetic and controls offspring at P7 and P21. However, the offspring of diabetic dams presented inferior weight during the infancy period being insulin treatment to the dam able to fully prevent this alteration at P7, but only partially at P21. Maternal diabetes also delayed the offspring eye opening day when compared to controls. Interestingly, insulin treatment of the diabetic dams anticipated eye opening of the pups comparing to control, suggesting increased maturation.

At a molecular level, the content of synaptic proteins was not altered in the offspring of diabetic dams when compared with controls at P7 and P21. However, in the female offspring of diabetic dams, there was a tendency for reduced synapsin levels at P7. The number of

retinal ganglion cells (RGCs) was not affected by maternal diabetes and the number and morphology of microglia cells did not suffer major changes at both timepoints.

In terms of retinal structure, maternal diabetes induced a reduction in the photoreceptor inner and outer segments layer in both males and females and a reduction in the thickness of the combined nerve fiber layer (NFL), ganglion cell layer (GCL) and inner plexiform layer (IPL), at P21, but only in females. This effect was unrelated with ganglion cell loss and was prevented by insulin administration to the diabetic dams. Regarding retinal function, maternal diabetes induced a decrease in amplitude of flicker's 1st harmonic and in the scotopic b-wave in male offspring, indicating cone and bipolar cell dysfunction, respectively, being insulin treatment able to prevent the alterations. Female offspring of diabetic dams appear to be resilient to alterations in retinal neuronal function. Nevertheless, cone arrestin protein levels were decreased, an effect prevented by insulin administration and not observed in male offspring of diabetic dams.

Summarizing, the exposure to hyperglycemia during pregnancy delays eye opening day, suggestive of impaired development, and negatively impacts the offspring retina, namely, by inducing a thinning of several retinal layers with evident impact in terms of bipolar cell and photoreceptor function in males, and a reduction in arrestin levels in females. The results show a high susceptibility of photoreceptors to hyperglycemia, being these neurons particularly vulnerable to maternal diabetes, while insulin administration is able to prevent these alterations.

This work provided some insight that was missing about the impact of maternal diabetes in the developing retina and may inspire future developments in elucidating the mechanisms behind the observed alterations. This work highlights the importance of evaluating the retina of children exposed to maternal diabetes particularly at infancy and also throughout life, emphasizing the relevance of insulin therapy, while drawing the attention for the importance of considering sex-specificities in preclinical studies.

Keywords: Maternal diabetes, Retina, Neurodevelopment, Synapse, Microglia, Sex differences

GRAPHICAL ABSTRACT

Graphical abstract resuming the animal model used, methods and main results at P7 and P21, discriminating sex differences. Dashed arrows represent tendencies.

The results are expressed by alterations in STZ and STZ+INS offspring in comparison with CTRL.



SCIENTIFIC COMMUNICATIONS

Filipa I. Baptista, Raquel Boia, Beatriz Paiva, Rita Gaspar, **Margarida Realinho**, Raquel Correia and António F. Ambrósio. Maternal Diabetes impacts offspring retinal structure and function. Poster presented at the XVII Meeting of the Portuguese Society for Neuroscience. Coimbra, December 1-3, 2021

Filipa I. Baptista, Raquel Boia, Beatriz Paiva, **Margarida Realinho**, Raquel G. Correia, António F. Ambrósio. Impacto da diabetes materna na estrutura e função da retina dos descendentes. Poster presented at “18th Annual meeting of the Portuguese Society of Diabetology”. Vilamoura, Portugal. March 10-12, 2022.

Margarida Realinho, Raquel Boia, Beatriz Paiva, Rita Gaspar, Raquel Correia, António F. Ambrósio and Filipa I. Baptista. Maternal Diabetes impacts offspring retinal structure and function. 4th Retreat of CIBB's Neuroscience and Disease Area. Coimbra, May 20, 2022.

Chapter 1: Introduction

1.1. Anatomy of the retina

The eye is a fundamental structure of the visual system being divided in three main layers: the sclera, the choroid, and the retina, which is part of the CNS (Figure 1). The retina is responsible for photosensitive functions and is organized in layers consisting mainly in 5 types of neurons: photoreceptors, bipolar cells, horizontal cells, amacrine cells and RGCs. In the outermost part, just before the choroid, there is a monolayer formed by cuboid pigmented epithelial cells, the retinal pigment epithelium (RPE). The RPE is responsible for the absorption of the light that is not absorbed by photoreceptors, and also for the phagocytosis of the outer segments of photoreceptors. Photoreceptor segments constitute the inner/outer segment layer (IS/OS) of the retina, whereas their nuclei form the outer nuclear layer (ONL). The photoreceptors form synapses with bipolar and horizontal cells in the outer plexiform layer (OPL), while the inner nuclear layer (INL) is constituted by the nucleus of horizontal, amacrine, Müller and bipolar cells. The inner retina is constituted by the IPL where bipolar cells form synapses with RGCs and amacrine cells, and by GCL consisting in the cell bodies of the RGCs and displaced amacrine cells. The NFL is composed of the axons of RGCs (Field & Chichilnisky, 2007; Reese, 2011) (Figure 2).

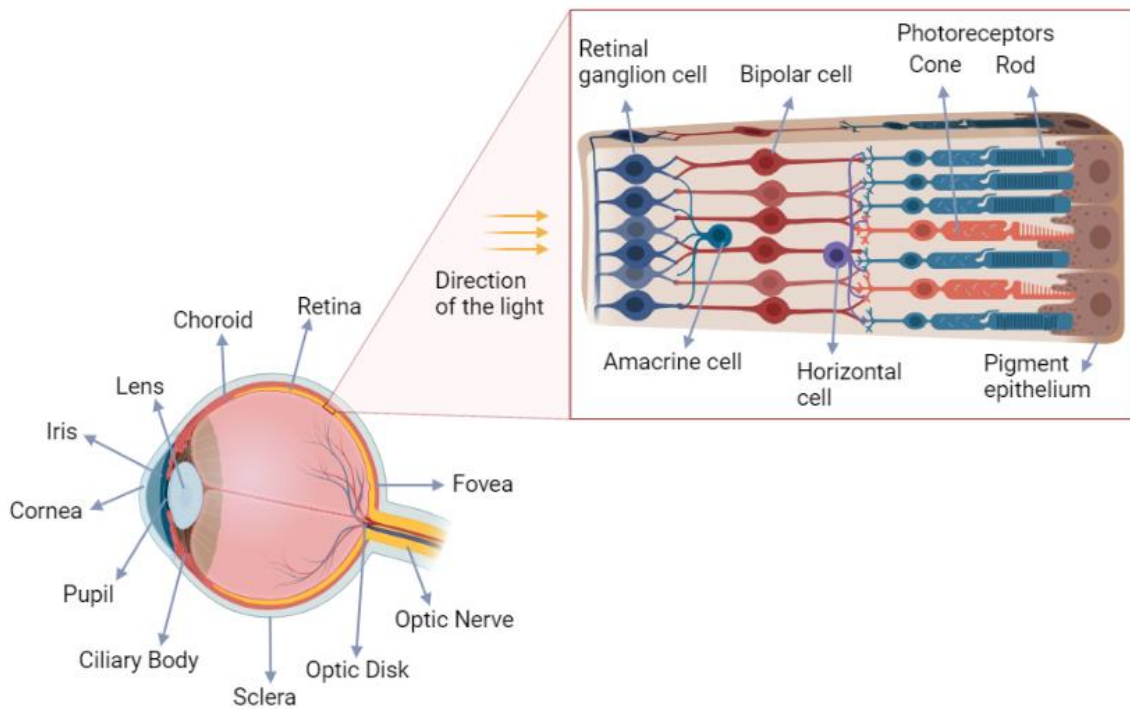


Figure 1: Anatomy of the eye. The retina is the most internal layer of the eye, covering its posterior side. The light enters the retina reaching the GCL first. However, it is in the photoreceptor's layer that the light energy is transformed in electrical energy and then synapsed onto bipolar cells and RGCs, consecutively. Created with BioRender.com.

There are two types of photoreceptors: rods and cones (Field & Chichilnisky, 2007). Light energy of the image being processed is transformed in electrical energy by the photoreceptor cells and vertically synapsed onto bipolar cells. These signals reach the RGCs that carry information to the brain via optic nerve. Horizontal cells modulate this information at the level of synapses between photoreceptor and bipolar cells, and amacrine cells at the level of synapses between bipolar cells and RGCs (Collin, 2008).

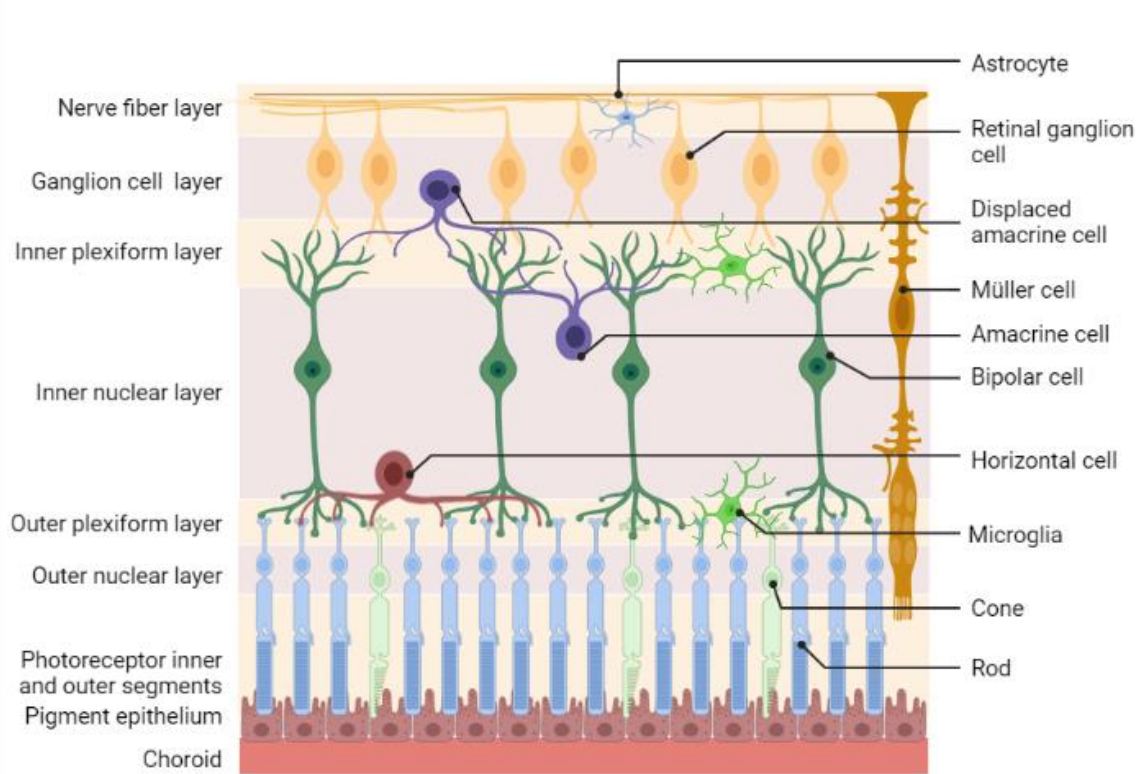


Figure 2: Schematic figure of the anatomy of the retina. The different types of cells are distributed through the organized layers of the retina. Created with BioRender.com.

Besides neurons, there are glial cells in the retina, namely Müller cells, astrocytes, and microglia. Müller cells stretch radially across the thickness of the retina, but their cell bodies sit in the INL. They have multiple functions such as maintaining the neuroretinal architecture, supplying end products of anaerobic metabolism, mopping up neural waste products and protecting neurons from exposure to excess neurotransmitters (Bringmann et al., 2006). Astrocytes enter the developing retina from the brain and are almost entirely restricted to the NFL. Their processes envelop RGCs axons and blood vessels, having a strong relationship with the blood-retinal barrier (Tao & Zhang, 2014). Microglial cells are immune cells with important roles both in retina development (Li et al., 2019) and in retinal degenerative processes (Madeira et al., 2015). The role of these cells will be further described in the next sections.

1.2. Retina development

1.2.1. Overview

Retina development is a complex process that culminates in the ability to perform visual transduction, passing visual signals from photoreceptor cells to RGCs, via interneurons such as bipolar, horizontal and amacrine cells. RGCs axons then carry the information from the retina to the brain via optic nerve (Collin, 2008).

During retina development in vertebrates, the different types of cells have different periods of differentiation (Figure 3). RGCs are the first cell type to differentiate, followed by horizontal cells and cones, while amacrine cells, rods, bipolar cells and Müller glia are produced progressively later (Reese, 2011).

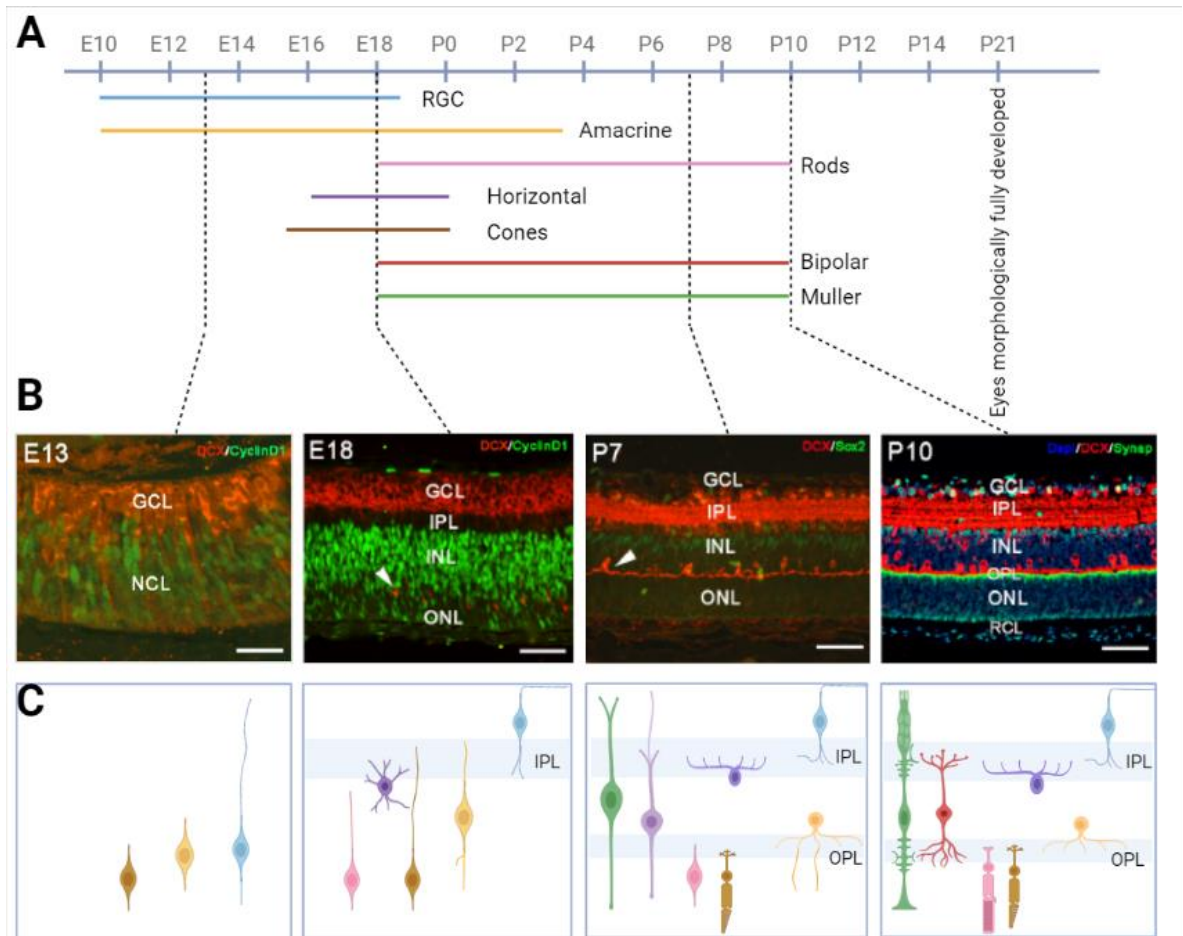


Figure 3: Time course of mice retinal development. (A) Periods of birth of each cell type (adapted from Telegina et al., 2021). **(B)** Immunolabeled images of specific time points in mice development (Fan et al., 2016). **(C)** Schematic images of the cells disposition and morphology over the same time

points (adapted from Reese, 2012). The color scheme used on the cells is the same in figure A and C. Created with BioRender.com.

P0–P14 represents a critical period of rodent retinal development since almost all neurons differentiate during this timeframe. Fan et al. (2016) described the process in mice as it follows:

- On embryonic day 13 (E13), the cornea, lens, and retina can already be identified in the eyeball. The retina consists of RPE and a retinal nerve layer (outer retina), separated by a narrow space. The outer retina is relatively thick and comprised numerous neural stem cell, forming the neuroblastic cell layer (NCL).
- Neural stem cells start to differentiate into neurons and to migrate into the GCL, later differentiating into RGCs on E13.
- With maturation, GCL gets thinner and becomes a single layer, while the IPL gets wider.
- At E18, some neural cells in the NCL began to differentiate into horizontal cells which separates the NCL in two zones, the INL and the ONL, divided by the OPL, consisting in numerous axons of photoreceptors and dendrites of horizontal cells and bipolar cells.
- At P7, neural stem cells in the ONL and INL are almost absent. The zone between the ONL and the RPE is occupied by the dendrites of photoreceptors.
- Still at P7, the cell bodies of horizontal cells are located near the edge of the INL, but their dendrites stretch into the OPL. Bipolar cells are located within the INL, with their cell bodies initially arranged in multilayers in the ONL near the OPL. Their dendrites extended into the OPL, and their axons stretch into the IPL and connect with RGCs. After P14, bipolar cell number increases, and they are arranged densely with typical morphology. Photoreceptors become mature also presenting their typical ultrastructure.

1.2.2. Synaptogenesis

Synapses of the mammalian CNS are asymmetric sites of cell–cell connection between nerve cells and their assembly involves a complex interplay of cell–cell adhesion, inter-neuronal signaling and site-specific recruitment of macromolecular protein complexes (Garner et al., 2002). This process of formation of connections between neurons is called synaptogenesis.

Synaptogenesis is a complex process that involves signaling on both sides of the synapse-to-be. It is thought that the initial synapse formation is due to a transient and nonspecific contact that may be mediated by the combined action of multiple cell adhesion molecules. Afterward, synapses are validated and stabilized by many activity-dependent processes.

In the brain, synapsin and synaptophysin, major synaptic vesicle proteins, are expressed even before the axon fully differentiates. After differentiation they accumulate in the distal axon and neuronal growth cone. When the axon contacts an appropriate target, synapsin and synaptophysin form large puncta of immunoreactivity corresponding to vesicles within presynaptic specializations (Fletcher et al., 1991). Due to this fact, synapsin and synaptophysin protein levels analysis is widely used to investigate synaptogenesis progress.

At the postsynaptic membrane there is a high concentration of glutamate receptors, associated signaling proteins, and cytoskeletal elements, all assembled into an organized structure called the postsynaptic density (PSD), which dynamically changes its structure and composition during development and in response to synaptic activity (Sheng & Hoogenraad, 2007). PSD-95, a scaffolding protein present at PSDs, is used to label glutamatergic postsynaptic sites (Morgan et al., 2008)

In the retina, synapses occur in two specific synaptic layers, the OPL, where photoreceptors form synapses with horizontal cells and bipolar cells, and the IPL, where synapses are formed between bipolar cells, amacrine cells and RGCs (Fan et al., 2016).

On the embryonic and early postnatal days, before synapse formation in the retina, synaptophysin was found only in the processes of photoreceptors, especially in the outer segment, being at P5, densely localized at the ends of inner segments of photoreceptors. At P7, synaptic connections are formed between the inner segments and horizontal cells. From P10 forward, synaptophysin was no longer localized in photoreceptors' processes, but specifically in presynaptic terminals. After P14 the synaptophysin-positive presynaptic terminals are concentrated densely in the OPL and IPL (Fan et al., 2016).

Synaptogenesis in the mouse retina occurs mostly from P5 to P14, along with the development of the retinal neural circuitry. The day of eye opening in mice is usually around P14, when the retinal architecture is formed and ready to proper visual function at the time of eye opening (Fan et al., 2016).

1.2.3. Synaptic transmission

Retinal synaptic contacts can be excitatory, inhibitory, or modulatory, but the majority is excitatory and uses glutamate as a neurotransmitter. Inhibitory neurotransmission is mediated by GABA and glycine, and modulatory neurotransmission is mediated by noradrenaline, serotonin, dopamine, acetylcholine and neuropeptides. Generally, presynaptic bouton from a given neuron only release neurotransmitter of one type, but they usually receive multiple forms of synaptic inputs (Garner et al., 2002).

Glutamate is the neurotransmitter for rod and cone photoreceptors, bipolar cells and RGCs, while GABA is the neurotransmitter for a subpopulation of horizontal cells, some amacrine cells and perhaps a small population of RGCs. Glycine is the neurotransmitter for a

subpopulation of amacrine cells. Information processing in the vertebrate retina is predominantly mediated by synapses using these amino acids (Wu & Maple, 1998).

Despite fully formed, the retinal synaptic network continues to mature and to be refined after eye opening in mammals. The development of RGC dendritic ramification and synaptic connections undergoes a dramatic activity-dependent remodeling. Visually evoked activity modulates the formation of retinal synaptic pathways, particularly ON and OFF pathways, at RGC level (Tian, 2004).

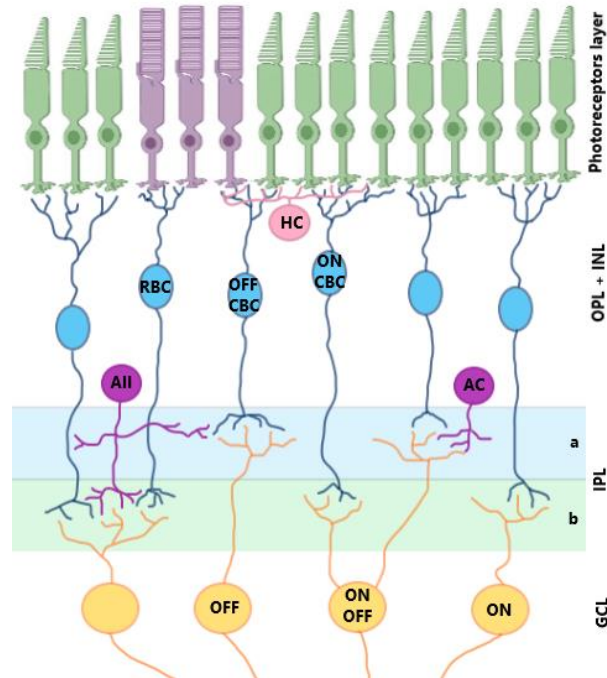


Figure 4: Cellular structure of the retina, showing the ON and OFF pathways. AC, amacrine cell; All, All amacrine cell; HC, horizontal cell; Off CBC, cone-driven OFF bipolar cell; On CBC, cone-driven ON bipolar cell; RBC, rod-driven bipolar cell. Created with Paint 3D.

These ON and OFF pathways are responsible for separating the visual image in different components, to be interpreted in the brain visual centers (Figure 4). This division in components starts at the photoreceptor level. Rods deal with dim signals of slowly varying brightness and cones with bright signals and rapidly varying light fluctuations. Rods and cones establish synapses with bipolar cells that are divided in different types, each with a different response to photoreceptors glutamate stimulus. An example of this difference in responses is that some bipolar cells have excitatory glutamate receptors and others have inhibitory receptors, leading to OFF and ON responses, respectively, initiating a set of parallel visual pathways for shadow and for highlight detection (Nelson & Kolb, 1995).

At the RGCs level, the separation between ON/OFF pathways relies on synapses between bipolar and RGCs in different layers of the IPL, the sublamina a and sublamina b: ON RGCs synapse with ON bipolar cells in sublamina b, OFF RGCs with OFF bipolar cells in sublamina a, and ON-OFF RGCs synapse with both, signaling both the onset and termination of light stimulus (Famiglietti Jr & Kolb, 1976). The rod-driven bipolar cells do not directly synapse with RGCs. Instead, they synapse with All amacrine cells and depolarize these cells when light is on (Bloomfield & Dacheux, 2001).

1.2.4. Role of microglia

The retina is considered part of the CNS and there are various similarities to the brain also regarding the development processes and the involvement of microglia in those processes.

Microglia, the resident brain macrophages, comprises 5-10% of total CNS cells and are the first tissue macrophages to be born, approximately at E8.5-E9.5 in the mouse, having critical roles in CNS development. Microglia have a role in initiating cell death and engulfing dead or dying cells in the mammalian brain. Microglia also express neurotransmitter receptors and are dynamic sensors of neural activity, suggesting key roles in the formation and remodeling of neural circuits, namely through synaptic pruning, consisting in eliminating unnecessary synapses. Lastly, microglia abnormalities like the increase in immunoreactivity and mutations in microglia related genes are associated with a range of psychiatric disorders, such as autism, schizophrenia and bipolar disorder (Frost & Schafer, 2016).

Fractalkine signaling pathway involving the ligand CX3CL1, expressed by neurons, and its receptor CX3CR1, that is exclusively found on microglia, plays an essential role in regulating the development and plasticity of neuronal circuits with functional consequences on the brain connectivity, neurogenesis, learning and memory, and the behavioral performance. There is a strong evidence suggesting that CX3CR1 signaling between microglia and neurons is involved in processes as the survival of newborn neurons, the maturation and elimination of synapses, the regulation of synaptic transmission, long term synaptic plasticity, and adult hippocampal neurogenesis (Paolicelli et al., 2014).

In the mouse retina, microglial cells are present in the retina as soon as at E11.5 and they are thought to appear in two distinct waves. The first one occurs before vascularization, proceeding from the vitreous surface of the retina or migrating from nonneuronal ciliary regions in the periphery. The second wave of infiltration occurs after blood vessel formation, where microglia invade the retina from the optic disc or via blood vessels themselves. At E17, 99% of microglia localize in the IPL. At P3 they become present at the GCL and at P9 within the developing OPL (Figure 5). The adult OPL contains about 47% of the microglial population while 53% are found in the IPL, suggesting a correlation with the development of retina synapses (Li et al., 2019). The number of microglial cells increase during the first postnatal

week and decrease thereafter until the retina circuit is considered mature (Santos, Ana M., Calvente et al., 2008).

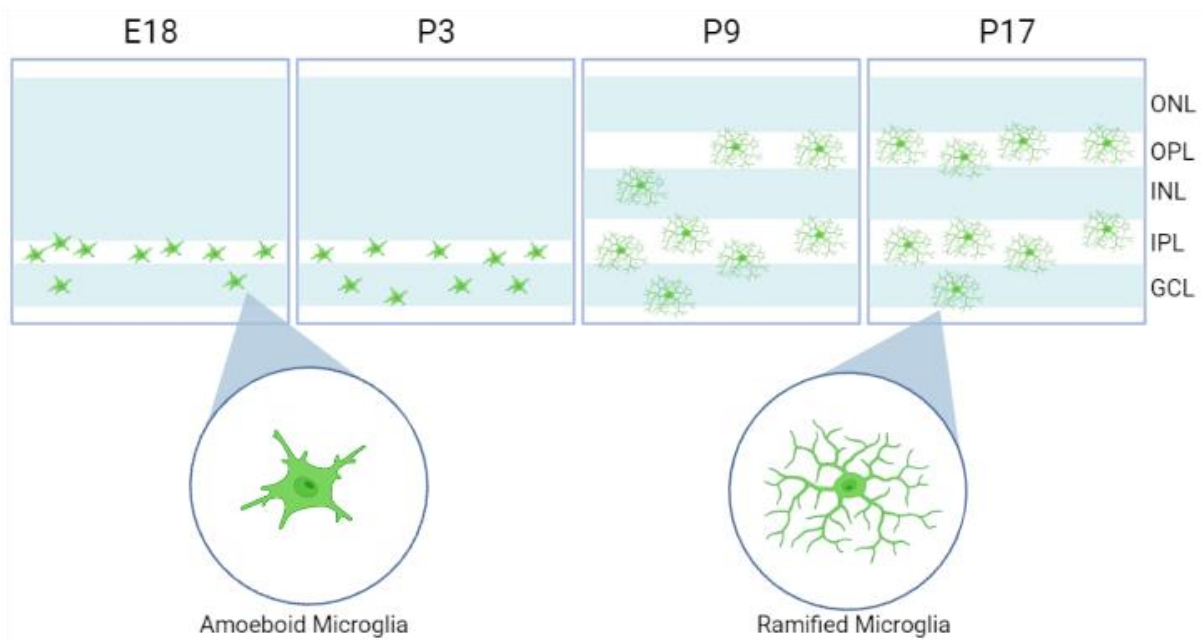


Figure 5: Distribution of microglia in the developing rodent retina and schematic representations of amoeboid versus ramified morphology. Created with BioRender.com.

In fact, the role of microglia in the retina appears to be analog to what is described in the brain. During retina development, microglia was shown to have an impact on blood vessel formation (Checchin et al., 2006), mediating apoptosis of vascular endothelial cells (Lobov et al., 2005), supporting and guiding the process of proliferation and even regulating astrocyte numbers (Puñal Id et al., 2019). Microglia presence also appears to be required for normal retinal growth and neurogenesis, being involved in microglia-mediated phagocytosis of neurons, synapse refinement and pruning (Li et al., 2019).

Another microglia characteristic that is important to note is that its morphology seems to be related with functional states. In newborn and early postnatal rats, the microglia were shown to have a rounder shape with pseudopodal processes, a shape known as amoeboid. As animals age, the cell bodies become progressively smaller and the processes longer and thinner. These ramified microglia actively retract and extend their processes, monitoring neurons, and engaging in metabolite removal and clearance in the CNS. Amoeboid microglia are considered an activated form, strongly involved in development and remodeling of neural tissue and containing numerous lysosomes and phagosomes (Li et al., 2019).

1.3. Diabetes mellitus

Diabetes mellitus is a set of metabolic disorders consisting in chronic hyperglycemia caused by defects in insulin secretion (which leads to low levels of insulin), defects in insulin action (characterized by insulin resistance of target tissues), or a combination of both (Kharroubi, 2015).

Diabetes can be classified in T1D, Type 2 (T2D), Gestational Diabetes (GDM) and other specific types that will not be discussed here. Focusing on the three major classifications, T1D results from cellular autoimmune pancreatic beta-cell destruction, leading to absolute insulin deficiency. This type has also been known as insulin-dependent diabetes. T2D is referred to as noninsulin-dependent and is characterized by relative insulin deficiency or insulin resistance. As for GDM, it is characterized by diabetes with onset or first recognition during pregnancy (Schuster & Duvuuri, 2002).

1.3.1. Diabetes in pregnancy

Pregestational and GDM prevalence has been increasing (Ferrara, 2007), and in 2017 it was estimated that 16.2% of all births worldwide were affected by hyperglycemia, 86.4% due to GDM. This is associated with adverse pregnancy and neonatal outcomes (Dickens & Thomas, 2019).

Fetal growth and development are greatly dependent on the capacity of the mother to supply nutrients and on the ability of the placenta to transfer these nutrients to the fetus. An abnormal intrauterine environment, such as in a diabetic condition characterized by an increased placental transport of glucose and other nutrients from the mother to the fetus, can cause a disturbance in fetal growth (Van Assche et al., 2001).

In humans, increased birth weight is common in infants of diabetic mothers (Aerts et al., 1990), implicating birth complications such as a higher risk of cesarean delivery, shoulder dystocia and birth injuries (Szmuiłowicz et al., 2019). Some of the metabolic effects found on rats such as neonatal hypoglycemia, hypocalcemia, hypomagnesemia and asymmetric macrosomia were also found in humans (Schwartz & Teramo, 2000).

Dietary advice, blood glucose monitoring, and insulin therapy were shown to reduce the incidence of primary composite outcome of infant death, shoulder dystocia, bone fracture, and nerve palsy by 67%, and reductions in average birthweight and rates of macrosomia were also noted (Johns et al., 2018).

In an animal model of T1D during pregnancy, it was shown that from P7 to P21, the offspring of T1D dams presented an inferior weight compared with control offspring, and that insulin administration to the dams was able to prevent this, resulting in a superior body weight in female offspring (Sousa et al., 2020).

When dams have severe diabetes, the fetuses are confronted with very high glucose concentrations, inducing islet hypertrophy and β -cell hyperactivity, which may result in early hyperinsulinemia. However, because the secretion of insulin is faster than its biosynthesis, β -cells become depleted and the exhaustion results in fetal hypoinsulinemia. When the mother has mild diabetes, the fetuses experience hypertrophy of the endocrine pancreas and hyperplasia of the β -cells and insulin response is increased. At adulthood, the offspring display a normal mass of endocrine pancreas but on glucose stimulation insulin response is deficient (Van Assche et al., 2001).

On offspring of experimentally diabetic rats, induced by STZ injection on the first day of gestation, it was found that diabetes of the mother during pregnancy induced alterations in fetal metabolism with persisting consequences in later life. Those alterations include hyperglycemia, hyperinsulinemia, macrosomia or microsomia (in mild diabetes and severe diabetes, respectively), altered β -cell response and amino acids metabolism, insulin resistance and increased risk of developing GDM (Aerts et al., 1990).

The incidence of abnormalities in several systems is increased in the presence of maternal diabetes, and in particular in the CNS (Schwartz & Teramo, 2000), which will be discussed in the next section.

1.3.2. Impact of maternal diabetes on offspring CNS

There are several evidences demonstrating that the offspring CNS is affected by maternal diabetes, leading to lower school scores and IQ in infancy and adolescence periods (Fraser et al., 2012; Nahum Sacks et al., 2016), expressive language impairments in infancy (Dionne et al., 2008) and a higher risk for long-term neuropsychiatric morbidities (Nahum Sacks et al., 2016).

Offspring of diabetic mothers also suffer from an increased risk of impaired neurodevelopmental outcomes in several aspects such as memory and facial recognition. The risk of developing autism spectrum disorders and schizophrenia has also been documented (Szmilowicz et al., 2019; Van Lieshout & Voruganti, 2008).

In animal models of GDM, behavioral alterations also occur, with offspring of diabetic dams showing inattentive behavior and recognition memory impairment (Vuong et al., 2017). Diabetes during pregnancy also impairs short-term memory specially in female offspring, demonstrated with behavioral tests (Kinney et al., 2003; Sousa et al., 2020). Moreover, offspring exposed to diabetic environment in fetal life can show anxiogenic/emotional behaviors in adulthood (Ramanathan et al., 2000). GDM was shown to induce chronic inflammation on the brain, with an increase in amoeboid microglia and levels of inflammatory cytokines (Vuong et al., 2017). The levels of some neural and synaptic markers were also altered in offspring of diabetic dams, which suggests changes in neuronal function and at

synaptic level. This is the case of synaptophysin, which immunoreactivity was reduced in the hippocampus, (Vafaei-Nezhad et al., 2016). The levels of fractalkine receptor (CX3CR1), important in the crosstalk between microglia and neurons, neuronal nuclear protein (NeuN), a marker of mature neurons, and vesicular glutamate transporter protein (VGLUT), which is present at glutamatergic synaptic vesicles, were also reduced in offspring of diabetic dams, especially in males, while insulin treatment prevented these alterations (Sadeghi et al., 2018; Sousa et al., 2020). All these findings can be correlated with physiologic changes induced by hyperglycemia exposure.

Despite the evidence that maternal diabetes affects the offspring brain, little is known about its impact on the retina. However, because the retina is part of the CNS, it is plausible that it may be affected as well.

1.3.3. Impact on the developing retina

One piece of evidence that sustains the hypothesis that retina development might be affected by gestational hyperglycemia is the fact that rat offspring of diabetic dams show a delay in eye opening, an important development hallmark. This may imply that the retina is not fully developed by the expected time. Insulin administration to diabetic dams not only prevented this effect but also anticipated eye opening (Sousa et al., 2020; Valente Piazza et al., 2019).

In humans, some of the findings include changes in retina morphology such as thinning of the pericentral macular parameters in children from diabetic pregnancies, similar to the retinal thinning observed in individuals before the onset of diabetic retinopathy, which suggests implications on the developing neurologic system of the fetus (Tariq et al., 2010). Additionally, female sex, short gestation time, low birth weight, and poor maternal diabetes control have also shown to increase the risk of developing segmental optic nerve hypoplasia, also called topless disks (Landau et al., 1998).

In a rodent animal model, it was shown that uncontrolled diabetes during pregnancy reduces the number of RGCs and increases the number of apoptotic RGCs in the offspring at P28. Notably, it was observed an increase in total retina thickness, suggestive of vascular permeability of the offspring retinal vessels and neuroinflammation (Najafdari et al., 2014).

In GDM rat models, Müller cells were evaluated to understand if diabetes during pregnancy induces alterations in these retinal cells. It was shown that glial fibrillary acidic protein (GFAP) expression was increased in Müller cells, showing that glial cells may be affected and suggesting an impact on retinal microenvironment (Tabasi et al., 2017). In zebrafish embryos exposed to high concentrations of glucose, the eye morphology was also altered. The thickness of IPL was reduced and INL and GCL thickness increased. Retinal cell proliferation was diminished following exposure to hyperglycemia: RGC and Müller cells' number was reduced (Singh et al., 2019). In another study with zebrafish embryo exposure to elevated

glucose, it was also shown that there is a reduction in photoreceptors and horizontal cells number, with visual defects, exhibiting signs of reactive gliosis and elevated apoptosis. Even after return to normoglycemia, larvae showed a persistent decrease in cones number (Titalii-Torres & Morris, 2022).

1.4. Aims

It is well established that maternal diabetes negatively impacts the brain of offspring, giving rise to short- and long- term adverse effects. However, very little is known about its specific impact on the retina, which is part of CNS and is considered an extension of the brain.

Being the retina the neural portion of the eye, we hypothesized that diabetes during pregnancy adversely impacts on offspring retina development, leading to structural and functional deficits, which may account for visual problems at infancy possibly persisting until adulthood.

Specifically, we aim to evaluate the impact of maternal diabetes on retina development and offspring eye opening day, which is an indicator of neurodevelopment, and also on offspring retina structure and function focusing on infancy period.

Additionally, we also aim to clarify if males and females have a different vulnerability to hyperglycemia during development, since we have already described that maternal diabetes has a sex-specific impact in the offspring brain (Sousa et al., 2020). At the same time, we aim to address if the treatment of the dam with insulin is able to prevent any changes detected.

Chapter 2: Methods

2.1. Ethics statement

All animals were handled according to the European Community guidelines (2010/63/EU) for the use of experimental animals, translated to the Portuguese law in 2013 (Decreto-lei 113/2013). In addition, all procedures involving animals were conducted in accordance with the Association for Research in Vision and Ophthalmology (ARVO) Statement for the Use of Animals in Ophthalmic and Vision Research and were approved by the Animal Welfare Committee of the Coimbra Institute for Clinical and Biomedical Research (iCBR), Faculty of Medicine, University of Coimbra (ORBEA 01/2017).

All efforts were made to minimize the suffering and the number of animals used. Moreover, people working with animals have received appropriate certification by FELASA (Federation of Laboratory Animal Science Associations), as required by the Portuguese authorities.

2.2. Animals

Wistar female rats approximately 8 weeks of age, were used for mating. Prior mating the animals were kept 2 per cage under controlled temperature and humidity in cycles of 12h light/12h dark with access to water and food *ad libitum*. The females' weight was between 150-208g.

Diabetes was induced by an IP injection of STZ (45mg/kg) in 0.1 M sodium citrate buffer. STZ is a toxin that destroys pancreatic β -cells, inducing T1D.

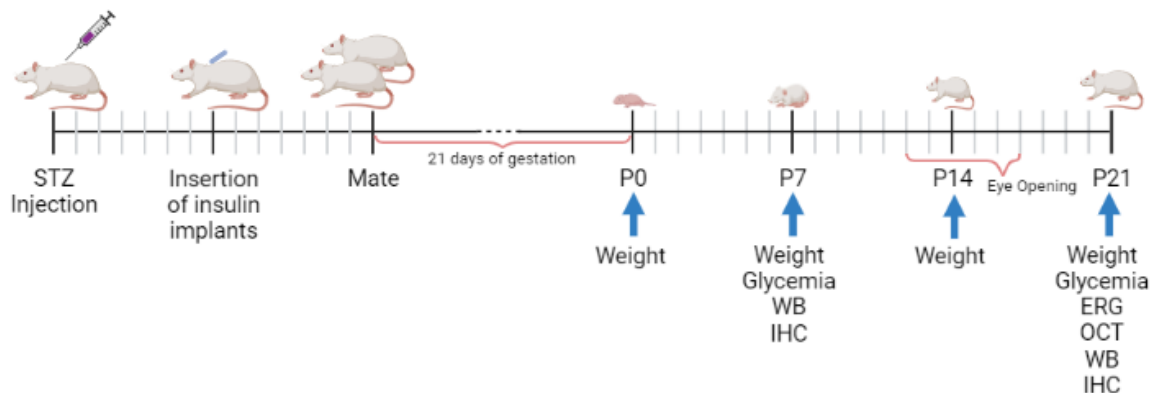


Figure 6: Schematic figure of the general timeline. Created with BioRender.com.

After diabetes onset a subset of STZ females received an insulin implant, whereas the remaining females received a blank implant (microcrystallized palmitic acid) of 7mm long and 2 mm diameter. The implant was inserted subcutaneously in the dorsal skin, with the animals previously anaesthetized with 2.5% isoflurane in O₂. A small orifice through the skin was created using a scalpel and a trocar and stylet were used to insert the implant. The area

of the skin, the instruments and the implant were all cleaned with a 10% povidone-iodine solution before the procedure.

The females were mated with non-diabetic males (1 male per 2 females) 1 week after diabetes onset (when blood glucose levels exceeded 250 mg/dL). Male and female offspring from CTRL, STZ and STZ+INS experimental groups were evaluated during infancy period (P7 and P21).

2.3. Weight and glycemia

The weight of the dams before any procedure and in the days after mating, to assess whether they were pregnant or not, was performed. The weight of the pups was carried out at P0, P7, P14 and P21.

Using a regular glucometer, glycemia values were measured before any procedure to get the basal values, and then 48 h after STZ administration. In the case of the pups, glycemia values were collected at P7 and P21.

2.4. Eye opening

Eye opening was monitored, with special attention between P12 and P17, by observation of pups and the percentage of pups with eyes opened, per litter, per day, was calculated.

2.5. Electroretinogram

The use of the ERG for assessment of retinal function has become a routine procedure in many medical centers throughout the world (Perlman, 1983). It consists of the sum of all retinal activity in response to light and is recorded from the corneal surface of the eye. In dark-adapted (scotopic) conditions, the flash ERG has a characteristic waveform, where the earliest component is a short-latency negative-going potential, the a-wave, followed by a positive-going potential, the b-wave. The rising phase of the b-wave shows oscillations, the oscillatory potentials (OPs) (Brandli & Stone, 2015), proposed to appear due to cells in the IPL, such as amacrine cells, bipolar cells or RGCs (Frishman, 2006; Wachtmeister, 1998).

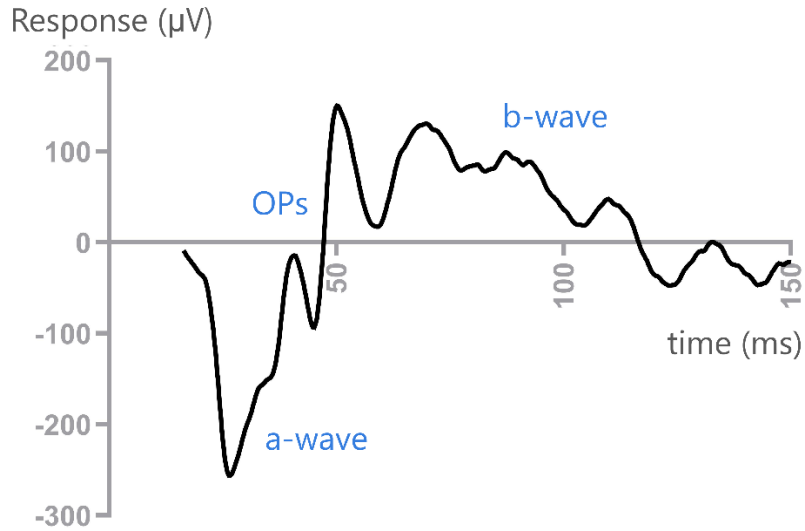


Figure 7: Dark adapted (scotopic) ERG showing the a-wave, b-wave and OPs. Created with Paint 3D.

In light adapted (photopic) conditions, the response differs because light stimulation in dark conditions activates rods' pathway while light stimulation in light adapted conditions activates cones. The curve has the same profile but with different wave amplitudes and in rats and mice the photopic ERG is devoid of a recordable a-wave (Figure 8) (Rosolen et al., 2008).

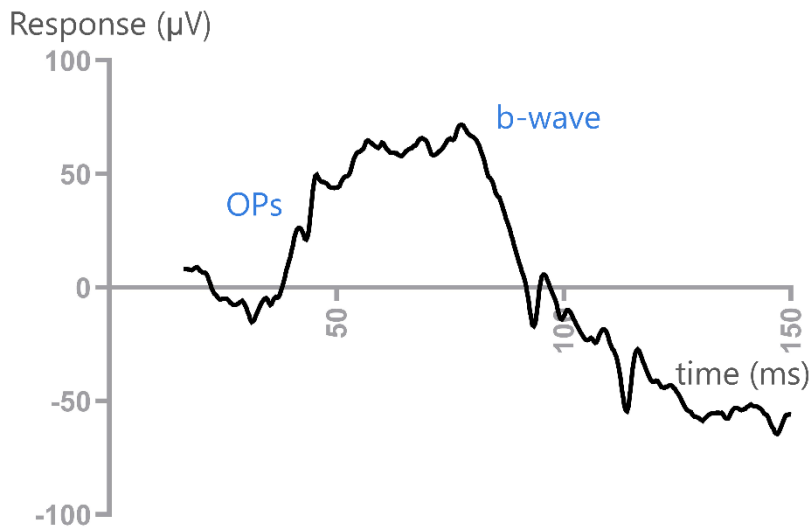


Figure 8: Light adapted (photopic) ERG showing the b-wave and OPs. Created with Paint 3D.

The a-wave is considered to be mainly generated by photoreceptors (Heynen & Van Norren, 1985). In scotopic conditions it reflects the responses of rods and cones because the flashes

of light are in the photopic range (Rosolen et al., 2008). The b-wave is mostly generated by bipolar cells (Massey et al., 1983; Sieving et al., 1994).

Other components of the ERG are the Scotopic Threshold Response (STR) and Flicker. STR is performed in the dark with a low intensity light stimulus and reflects predominantly the activity of RGC. STR response can be divided in two components, positive STR (pSTR) and negative STR (nSTR). pSTR has been shown to be more affected by chronic RGC damage and nSTR is more sensitive to acute lesions (Bui et al., 2013). The Flicker is performed in light adapted conditions and uses fast high intensity stimuli. It has two components, the first and second harmonic, which reflect cone response and middle to inner retinal contributions, respectively (Falsini et al., 1995; Frishman, 2006).

2.5.1. ERG recordings

ERGs were recorded in P21 pups after overnight dark adaptation of the animals. The animals were handled under dim red light and anesthetized by IP injection of ketamine hydrochloride (50 mg/kg; Nimatek, Dechra, UK) and xylazine (10 mg/kg; Sedaxylan, Dechra, UK). Then, oxybuprocaine (4 mg/mL; Anestocil, Edol, Lisbon, Portugal), a topic anesthetic, was applied in the eye and the pupil was fully dilated using topical tropicamide (10 mg/mL, Tropicil Top, Edol, Portugal) drops. Lubricating eye drops composed of carmellose sodique (4 mg/0.4 mL; Celluvisc, Allergan, Dublin, Ireland) were used to keep the eyes moisturized and to maintain stable corneal potential through the recordings.

The electrical responses were recorded with a gold electrode placed at the cornea, two reference electrodes placed at the head (one for each eye) and a ground one in the tail.

The STR was the first to be recorded, using a 0.000095 cd/m^2 light stimulus from a Ganzfeld stimulator (Roland Consult GmbH, Brandenburg, Germany). Then, the scotopic ERG was recorded applying a series of white light flashes, from 0.003 to $9.49 \text{ cd}\cdot\text{s/m}^2$. After light adaptation of 16 min, the photopic ERG was recorded using the same stimulus but under white background light (25 cd/m^2). Lastly, the Flicker was performed using the three higher light intensities, 0.95 , 3.00 and $9.49 \text{ cd}\cdot\text{s/m}^2$, delivered 10 times at 6.3 Hz.

2.5.2. ERG analysis

Using RETIport (Roland Consult GmbH, Brandenburg, Germany) software, the data corresponding to each exam, the amplitudes of pSTR and nSTR, scotopic a-wave and b-wave, photopic b-wave and flicker 1st and 2nd harmonics, were extracted. In the STR and both b-waves, data was extracted after applying an off-line digital filter (high frequency cut-off of 50 Hz).

The values obtained were used to perform the statistical analysis and to plot representative waves.

2.6. Optical coherence tomography

OCT is a high-resolution, noninvasive technique that performs cross-sectional imaging of internal structures in biological tissues by measuring optical reflections. The system performs multiple longitudinal scans at several lateral locations in order to provide a two-dimensional map of reflection sites in the sample, in an analogous way to ultrasound B-mode (Huang et al., 1991).

OCT is currently used to analyze morphological changes that accompany disease progression in humans and animal models, providing *in vivo* images without potential artifacts caused by histological processing (Berger et al., 2014). We used OCT to measure the thickness of each retinal layer and the total retina thickness, as shown in Figure 9.

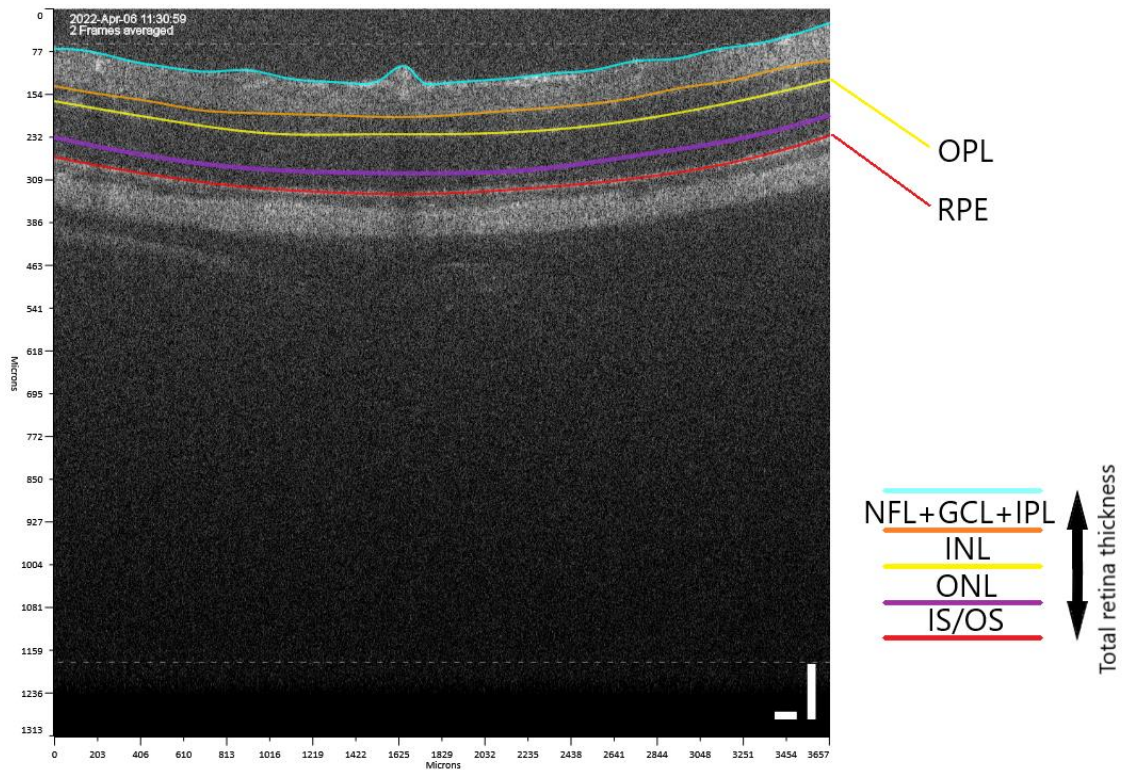


Figure 9: Typical OCT image of a P21 rat analyzed with Insight along with corresponding layers. The blue line corresponds to the anterior limit of the retina and the space comprised between the blue line and the orange one contains NFL, GCL and IPL. The yellow line corresponds to OPL, which marks the posterior limit of INL (situated between orange and yellow lines). ONL is delimited by the yellow line (OPL) and purple line. IS/OS layer is delimited by the purple line and the red one, which corresponds to RPE (posterior limit of the retina). Total retina thickness is considered between blue and red lines.

2.6.1. OCT recordings

The animals were anesthetized with an IP of ketamine hydrochloride (50 mg/kg; Nimatek, Dechra, UK) and xylazine (10 mg/kg; Sedaxylan, Dechra, UK) and data were collected from both eyes after corneal anesthesia with oxybuprocaine (4 mg/mL; Anestocil, Edol, Lisbon, Portugal) and pupil fully dilated using topical tropicamide (10 mg/mL, Tropicil Top, Edol, Portugal). Carmellose sodique (4 mg/0.4 mL; Celluvisc, Allergan, Dublin, Ireland) lubricating eye drops were also used to keep the eyes moisturized. For each eye 13 tomographic images were acquired as well as the respective fundus of the eye. The first image was centered on the optic nerve and the following scans were acquired in six scans above and six scans beneath that reference, scanning a total of 1700 μm of the eye and containing the retina.

2.6.2. OCT analysis

The images obtained were analyzed using InSight (Phoenix Research Labs, Pleasanton, United States) software. This software provides a semi-automatic segmentation of the retina considering the four layers described in Figure 9. The thickness can be measured and averaged afterwards.

2.7. Western Blot

2.7.1. Sample collection

At P21, offspring were anesthetized with 2.5% isoflurane (IsoFLO, Abbott Laboratories, Chicago, USA) in O_2 and sacrificed by decapitation. The eyes were enucleated and dissected to isolate the retinas. The resulting samples were frozen in liquid nitrogen and stored at -80°C .

2.7.2. Total extract preparation

Each retina was lysed in RIPA buffer supplemented with complete mini protease inhibitor cocktail tablets and 1 mM DTT, pH 7.2, at 4°C . After this, the lysates were processed in a sonicator to destroy the cells' membranes and were then centrifuged at 16,100xg for 10 min at 4°C . The supernatant was collected and stored at -80°C until use.

2.7.3. BCA protein quantification

A bicinchoninic acid (BCA) assay (Pierce Biotechnology, Rockford, USA) was conducted in order to assess protein concentration in each sample. This is a colorimetric assay consisting

of the use of a standard curve with a color degradation that is proportional to the quantity of protein present, in this case, albumin.

The samples were diluted in water and reagents A and B were added in a 50:1 proportion. Afterwards, the samples were tested against the albumin standard curve for absorbance, using BioTek absorbance microplate reader (BioTek Instruments, Winooski, United States) at a wavelength of 570 nm, to determine protein concentration.

After protein quantification, samples were denaturated by adding sample buffer and by boiling in a 95°C bath for 5 min to denature proteins.

2.7.4. SDS-PAGE western blot

Stacking (4%) and resolving (8%) sodium dodecyl sulfate (SDS) polyacrylamide gels were polymerized. Equal amounts of protein for each sample were loaded in the gels and the electrophoresis was conducted at 60 V for 15 min to allow the samples moving from the stacking gel to the resolving gel, and then at 150 V until proper protein separation.

After electrophoresis, electrotransfer was conducted from the gel to the polyvinylidene difluoride membranes, using CAPS with 10% methanol as the transfer buffer with an amperage of 0.75 A for 90 min.

The membranes were then blocked in 5% milk solution, before incubation with the primary and with the secondary antibodies coupled to alkaline phosphatase or horseradish peroxidase. Fluorescence/Chemiluminescence was detected using Typhoon/ImageQuant™ LAS 500 (GE Healthcare, Chicago, United States). Band intensity was quantified through ImageQuant™ software.

Table 1: Primary antibodies used for Western Blot.

Antibody	Type	Host	Supplier	Protein (µg)	Dilution	Observations
NeuN	Monoclonal	Rabbit	Abcam	10	1:5000	Neuronal nuclear marker
Synapsin-1	Monoclonal	Mouse	Synaptic Systems	10	1:1000	Presynaptic vesicle marker
PSD-95	Monoclonal	Rabbit	Cell Signaling	10	1:1000	Postsynaptic terminal marker
VGLuT1	Monoclonal	Mouse	Abcam	20 (not boiled)	1:1000	Glutamatergic synapse marker
VGAT	Monoclonal	Mouse	Synaptic Systems	20 (not boiled)	1:1000	GABAergic synapse marker
CX3CR1	Polyclonal	Rabbit	Abcam	10	1:1000	Fractalkine receptor marker
Rhodopsin	Monoclonal	Mouse	Sigma-Aldrich	10	1:1000	Rods' internal and external segments' marker
Arrestin	Polyclonal	Rabbit	Sigma-Aldrich	10	1:1000	Cones marker
Calnexin	Polyclonal	Goat	Sicgen	10	1:5000	Endoplasmic reticulum marker (loading control)

Table 2: Secondary antibodies used for Western Blot.

Antibody	Detection Method	Host	Supplier	Dilution
Anti-Mouse	Enhanced chemifluorescence (ECF)	Goat	Sigma	1:10000
Anti-Mouse	Enhanced chemiluminescence (ECL)	Goat	Bio-Rad	1:10000
Anti-Goat	ECL	Rabbit	Thermo Fisher Scientific	1:10000
Anti-Rabbit	ECF	Goat	Sigma	1:10000
Anti-Rabbit	ECL	Goat	Bio-Rad	1:10000

2.8. Immunohistochemistry

2.8.1. Sample collection and embedding

The animals were anesthetized with an IP injection of ketamine (80 mg/kg; Nimatek) and xylazine (5 mg/kg; 2% Ronpum) and transcardially perfused with phosphate-buffered saline (PBS) and then with 4% paraformaldehyde (PFA). The eyes were then enucleated and cleaned of surrounding tissues, always on ice. The eyes were then postfixed with 4% PFA for 1 h.

One of the eyes was processed for retinal cryosections and the other one for retina wholemounts as explained in the next section.

2.8.2. Cryosections and wholemounts tissue preparation

After incubation of the intact eye with PFA, a cut was performed in the cornea and the eye was incubated again with PFA allowing it to reach the inside. After 1 h PFA incubation, the eyes were immersed in a 15% sucrose solution and then in a 30% sucrose solution in PBS to cryoprotect the eye structures.

The eyes were then embedded in Optical Cutting Temperature compound (ThermoScientific, Waltham, USA) in cryomolds and positioned in the desired orientation. The samples were frozen by immersing the cryomold in dry ice. The frozen block was then marked to record the orientation of the optic nerve and wrapped in aluminum foil and stored at -80°C until needed.

For the wholemounts, the eyes were kept in PBS after the initial PFA incubation and stored at 4°C until use.

2.8.3. Sectioning using a cryostat

The cryostat temperature was defined to -20°C and the mold was set in the support. Retinal cryosections were cut (14 µm thickness) and placed on microscope slides, stored in -20°C until performing IHC experiment.

2.8.4. Immunohistochemistry of retinal cryosections

Before starting the immunostaining process, the slices were defrosted and let dry overnight at room temperature. The cryosections were fixed with acetone at -20°C for 10 min in coplin jars and then re-hydrated in PBS for 5 min, twice. Using a hydrophobic DAKOPen (DAKO, Glostrup, Denmark), the cryosections were circled to minimize the amount of antibody required. After pen drying for 1 min, the cryosections were permeabilized using a PBS-0.25% Triton X-100 (50 µL/section) for 30 min. After cells permeabilization, the sections were blocked in a 10% Goat serum-PBS-1% bovine serum albumin (BSA) (50 µL/section) for 30 min in a humidified plastic container.

After absorbing the blocking solution with paper, the cryosections were incubated with the primary antibodies in PBS-1% BSA (50 µL/section) in closed humidified plastic containers overnight at 4°C. The sections were then washed in PBS 3 times for 10 min each and incubated with the secondary antibodies (goat anti-rabbit Alexa Fluor 488 and goat anti-mouse Alexa Fluor 568; 1:500), and DAPI (1:5000; to stain cell nuclei) in PBS-1% BSA (50 µL/section) in plastic containers covered with aluminum foil for 1 h at room temperature.

Afterwards, the cryosections were washed with PBS 3 times for 10 minutes each, mounted with fluorescent mounting medium and frozen until image acquisition at the Fluorescence microscope.

Table 3: Primary antibodies used for cryostat slices immunostaining.

Antibody	Type	Host	Supplier	Dilution	Observations
Arrestin	Polyclonal	Rabbit	Sigma-Aldrich	1:500	Cones marker
Rhodopsin	Monoclonal	Mouse	Sigma-Aldrich	1:500	Rods' internal and external segments' marker

Table 4: Secondary antibodies used for cryostat slices immunostaining.

Antibody	Host	Supplier	Dilution
Anti-rabbit IgG Alexa Fluor® 488	Goat	Thermo Fisher Scientific	1:500
Anti-mouse IgG1 Alexa Fluor® 568	Goat	Thermo Fisher Scientific	1:500

2.8.5. Fluorescence immunostaining of wholemounts

Retinal wholemounts were washed with 0.5% Triton in PBS and frozen in the same solution at -80°C for 15 min. Afterwards, the wholemounts were defrosted, washed again and incubated with the primary antibodies in a solution of 2% Triton and 2% goat serum in PBS for 1 h at room temperature and then overnight at 4°C.

On the next day, the retina wholemounts were washed with 0.5% Triton in PBS and incubated with the secondary antibodies in the 2% Triton and 2% goat serum in PBS solution at room temperature for 2 h with agitation. DAPI was added in the secondary antibodies' solution in a 1:5000 dilution. Finally, the wholemounts were washed, mounted in microscope slides, and frozen until image acquisition.

Table 5: Primary antibodies used for wholemounts immunostaining.

Antibody	Type	Host	Supplier	Dilution	Function
Iba-1	Polyclonal	Rabbit	Wako	1:1000	Microglia marker
Brn3a	Monoclonal	Mouse	Millipore	1:500	RGC marker

Table 6: Secondary antibodies used for wholemounts immunostaining.

Antibody	Host	Supplier	Dilution
Alexa Fluor® 488 Anti-Rabbit IgG	Goat	Thermo Fisher Scientific	1:500
Alexa Fluor® Anti-Mouse IgG	Goat	Thermo Fisher Scientific	1:500

2.8.6. Image acquisition and analysis

Images from Iba-1 stained retinal wholemounts (P7 and P21) were acquired with a LSM 710 Meta confocal laser scanning microscope (Zeiss, Jena, Germany) with a 63x objective. Z-stack images were obtained to perform the tridimensional microglia reconstruction using the Neurolucida Software (MBF Bioscience, Williston, VT, USA). Morphometric data (branched structure analysis and Sholl analysis) was obtained in the Neurolucida Explorer and analyzed as explained in the next section.

Images from Brn3a stained wholemounts (P7 and P21) were acquired with a 20x objective in a single stack. Brn3a positive cells were counted using Image J software.

2.9. Microglia branched structure analysis and sholl analysis

Microglia number was assessed at P7 and P21 in retinal cryosections by counting the cells (number in total retina and per layer). Microglia morphology was assessed in retinal wholemounts by drawing 10 different microglial cells per animal, including both the cell body and processes using Neurolucida software. The parameters analyzed in the branched structure analysis were the number of branches per cell and per branch order, and the length of each branch per cell and per order. In the sholl analysis, each cell was analyzed considering several concentric circumferences of incremental 10 μm and the considered parameters were the number of times each circumference was crossed by a branch and the total length of branches present between two consecutive circumferences.

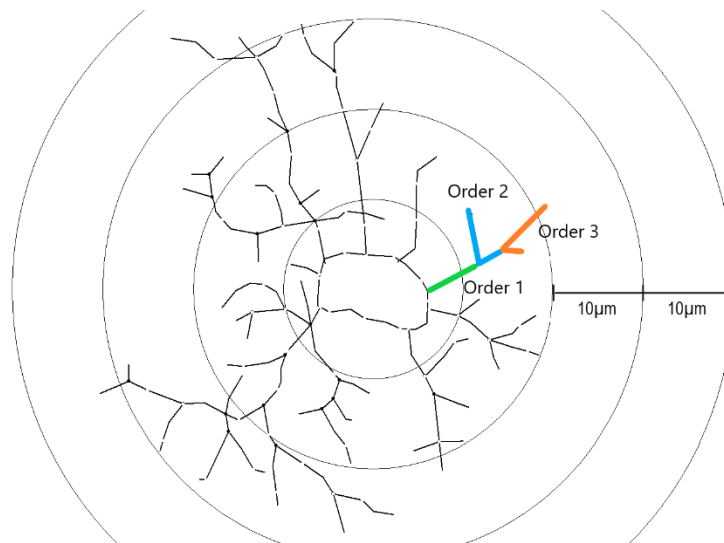


Figure 10: Schematic figure of a microglia cell analyzed with Neurolucida software. The colors represent different branch orders and the circumferences the incremental areas used in sholl analysis. Created with Paint 3D.

2.10. Statistical analysis

Outlier data values were excluded according to Graphpad Online Outlier Calculator (p -value=0.05). Statistical analysis was performed with Prism 8 (GraphPad Software) using one-way analysis of variance (ANOVA) or Kruskal-Wallis test in data-sets that do not assume a Gaussian distribution. P values less than 0.05 ($p < 0.05$) were considered significant. All values are presented as mean \pm standard error of the mean (SEM).

Chapter 3: Results

3.1.1. Metabolic characterization of the dams and litter size

Dams were weighted after mating (gestational day 0-G0) and before delivery day (G21). As expected, the weight of the dams increased between G0 and G21, but no differences were detected between control, diabetic and insulin-treated dams (Figure 11: A, B).

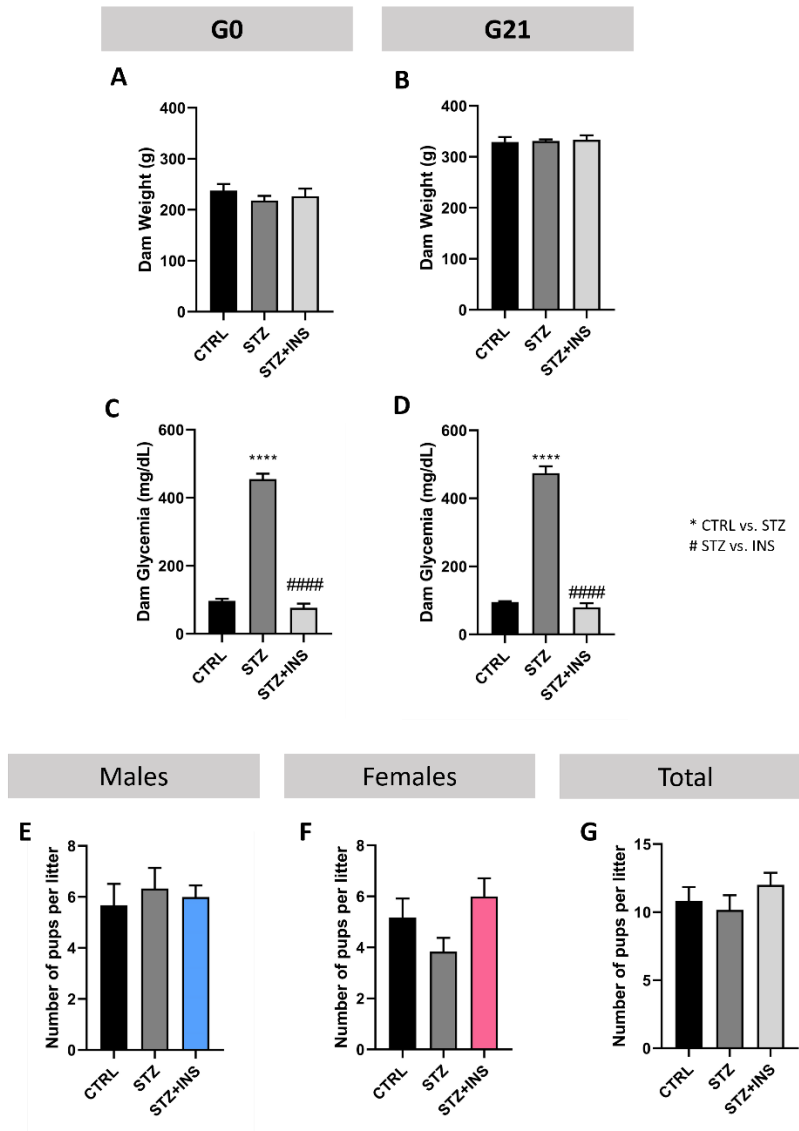


Figure 11: Dam bodyweight and glycemia at the beginning and end of gestation and number of pups per litter. Control dams' (CTRL) (black), diabetic dams' (STZ) (dark grey) and diabetic dams' treated with insulin (STZ+INS) (light grey) bodyweight, glycemia and number of pups per litter are presented as the mean \pm SEM. **(A)** Dam's weight at G0. **(B)** Dam's weight at G21. **(C)** Dam's Glycemia at G0. **(D)** Dam's Glycemia at G21. **(E)** Number of male pups per litter. **(F)** Number of female pups per litter. **(G)** Total number of pups per litter. For each of the three different experimental conditions 6 dams and litters were used. Statistical analysis was assessed with ANOVA or Kruskal-Wallis test in data-sets that do not assume a Gaussian distribution; **** $p < 0.0001$: STZ (grey) compared with CTRL (black) offspring; ##### $p < 0.0001$: STZ compared with STZ+INS (blue and pink) offspring.

On the same days, glycaemia levels were measured to assess normoglycemia in control and diabetic dams with insulin implant, and hyperglycemia in diabetic dams. The levels of glycemia did not change between G0 and G21 and untreated diabetic dams presented a statistically significant increase in glycemia compared to control and insulin treated ones on both time points (G0 – CTRL: 96.7 ± 6.8 mg/dL; STZ: 454.7 ± 16.0 mg/dL; STZ+INS: 76.3 ± 12.2 mg/dL; $p < 0.0001$; G21 – CTRL: 95.2 ± 2.55 mg/dL; STZ: 474.3 ± 19.8 mg/dL; STZ+INS: 79.5 ± 12.2 mg/dL; $p < 0.0001$) (Figure 11: C, D).

After pups' birth, each litter size was counted separating male and female pups. No differences in litter size were observed between control, diabetic, or diabetic dams treated with insulin.

3.1.2. Effect of maternal diabetes on offspring's bodyweight, glycemia and eye-opening day

It has been described that exposure to hyperglycemia during gestation can impact offspring metabolism and, consequently, bodyweight and glycemia levels. On the other hand, insulin administration to the dam has been shown to prevent these metabolic alterations (Aerts et al., 1990; Sousa et al., 2020).

To assess whether the impact of *in utero* exposure to hyperglycemia, pups were weight at early and late infancy (P7 and P21, respectively) and glycemia levels were measured (Figure 12).

In STZ male offspring, at P7, a significant decrease in bodyweight was detected when comparing to CTRL ($p = 0.02$) and STZ+INS ($p = 0.006$) male offspring (CTRL σ : 12.6 ± 0.5 g; STZ σ : 9.7 ± 1.0 g; STZ+INS σ : 13.1 ± 0.7 g). At P21, STZ male offspring remained with decreased bodyweight comparing with CTRL ($p < 0.0001$). Notably, at P21 insulin administration to the dams partially prevented STZ offspring bodyweight decrease, but not to similar values of CTRL, since STZ+INS pup weight was also decreased ($p < 0.0001$) when compared to CTRL (CTRL σ : 46.1 ± 1.0 g; STZ σ : 24.2 ± 1.5 g; STZ+INS σ : 36.4 ± 1.8 g).

In females, at P7, the weight of STZ offspring was tendentially reduced when compared with CTRL ($p = 0.07$) and significantly reduced ($p = 0.004$) when compared with STZ+INS (CTRL ♀ : 12.9 ± 0.4 g; STZ ♀ : 10.4 ± 1.3 g; STZ+INS ♀ : 14.2 ± 0.6 g). At P21, similarly to males, the differences between CTRL and STZ were accentuated ($p < 0.0001$) and the differences between STZ and STZ+INS were also detected ($p = 0.02$). STZ+INS females were also significantly lighter ($p = 0.006$) than CTRL offspring (CTRL ♀ : 42.5 ± 1.9 g; STZ ♀ : 24.1 ± 2.5 g; STZ+INS ♀ : 32.8 ± 1.8 g).

Concerning glycemia levels, no differences were found between CTRL, STZ or STZ+INS offspring, neither in males nor females.

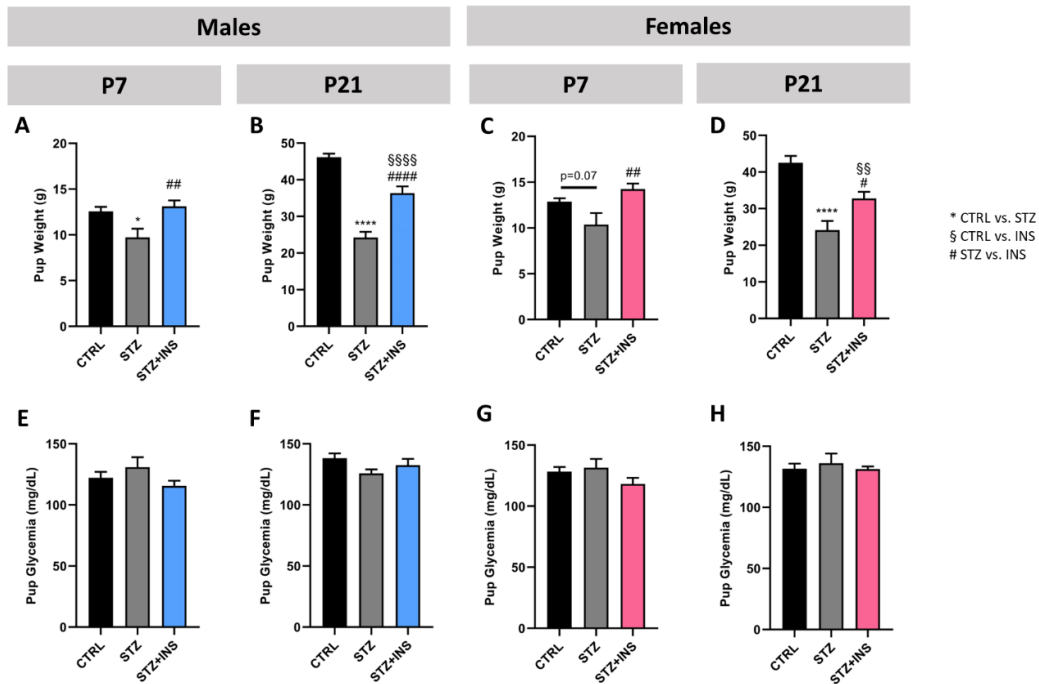


Figure 12: Effects of maternal diabetes in male and female offspring bodyweight and glycemia levels at early (P7) and late infancy (P21). (A) Male offspring bodyweight at P7. (B) Male offspring bodyweight at P21. (C) Female offspring bodyweight at P7. (D) Female offspring bodyweight at P21. (E) Male offspring glycemia at P7. (E) Male offspring glycemia at P21. (E) Female offspring glycemia at P7. (E) Female offspring glycemia at P21. The number of pups in each group (CTRL, STZ and STZ+INS) was between 10 and 14 in both sexes. Statistical analysis was assessed with ANOVA or Kruskal-Wallis test in data-sets that do not assume a Gaussian distribution; * $p < 0.05$, **** $p < 0.0001$: STZ (grey) compared with CTRL (black) offspring; §§ $p < 0.01$, §§§§ $p < 0.0001$: CTRL compared with STZ+INS (blue and pink) offspring; # $p < 0.05$, ## $p < 0.01$, #### $p < 0.0001$: STZ compared with STZ+INS offspring.

The day of eye opening was observed as an important pup developmental milestone. The percentage of pups with opened eyes per day was assessed (Figure 13). Both STZ males and females opened the eyes later than CTRL ones. At the same time, STZ+INS males and females opened the eyes sooner than CTRL ones. The differences were significant since P13, in males, when STZ+INS started to open the eyes before CTRL ($p = 0.02$) and STZ ($p = 0.02$) (STZ+INS σ : 25.0 ± 11.0 %). From P14 until P15 there were significant differences between the 3 groups ($p < 0.0001$ in all comparisons except for CTRL vs. STZ at P14, where $p = 0.001$), where every STZ+INS pup had open eyes and STZ pups had a lower percentage of open eyes compared with CTRL (P14 - CTRL σ : 14.2 ± 4.5 %; STZ σ : 0.0 ± 0.0 %; P15 - CTRL σ : 65.0 ± 5.9 %; STZ σ : 18.0 ± 5.5 %). By P16 both CTRL and STZ+INS had opened the eyes, unlike STZ which remained with a percentage of closed eyes until P18 ($p < 0.0001$; STZ σ : 58.3 ± 8.5 %).

In females, at P14, the percentage of eyes opened was significantly higher in STZ+INS when compared to both CTRL and STZ ($p < 0.0001$; CTRL♀: 12.0 ± 6.5 %; STZ♀: 0.0 ± 0.0 %; STZ+INS♀: 65.0 ± 10.0 %). At P15 the differences were significant between CTRL and STZ ($p = 0.0007$), CTRL and STZ+INS ($p = 0.002$) and STZ and STZ+INS ($p < 0.0001$) following the same pattern as in males (CTRL♀: 65.0 ± 8.2 %; STZ♀: 27.0 ± 8.2 %; STZ+INS♀: 100.0 ± 0.0 %). By P16 every CTRL and STZ+INS pup had open eyes, while STZ pups only by P18 ($p < 0.0001$; STZ♀: 44.0 ± 12.4 %).

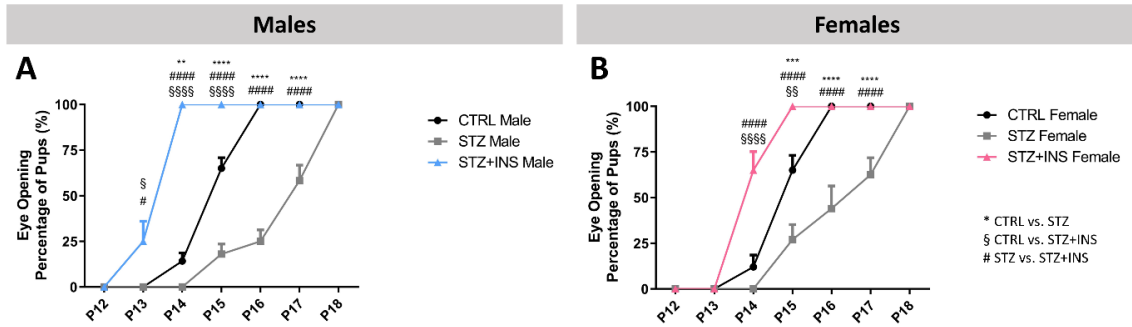


Figure 13: Diabetes during pregnancy leads to a delay in offspring eye opening, while insulin administration expedites it. (A) Percentage of male pups with eyes open per day. **(B)** Percentage of female pups with eyes open per day. We used 15 pups for each group and each sex. Statistical analysis was assessed with ANOVA or Kruskal-Wallis test in data-sets that do not assume a Gaussian distribution; ** $p < 0.01$, *** $p < 0.001$, **** $p < 0.0001$: STZ (grey) compared with CTRL (black) offspring; § $p < 0.05$, §§ $p < 0.01$, §§§ $p < 0.0001$: CTRL compared with STZ+INS (blue and pink) offspring; # $p < 0.05$, #### $p < 0.0001$: STZ compared with STZ+INS offspring.

3.2. Impact of maternal diabetes on offspring retina development at early infancy

3.2.1. Maternal diabetes does not induce changes in retinal synaptic and neuronal protein levels in male and female offspring at early infancy

Maternal diabetes may possibly impact offspring retina development by affecting neurons and microglia with repercussions in processes as neurogenesis and synaptogenesis. To assess molecular changes in offspring retina that may suggest synapse or neuronal alterations at early infancy, the protein levels of synapsin, PSD95, VGLUT1, VGAT and NeuN were assessed in retina total extracts (Figure 14), by Western Blot.

No significant differences were found between CTRL, STZ and STZ+INS males or females in any of the aforementioned synaptic proteins. Nevertheless, in STZ female offspring there is a tendency for lower synapsin protein levels when compared with CTRL (CTRL♀: 100.0 ± 8.4 ; STZ♀: 69.2 ± 5.6 ; $p = 0.07$) (Figure 14, B).

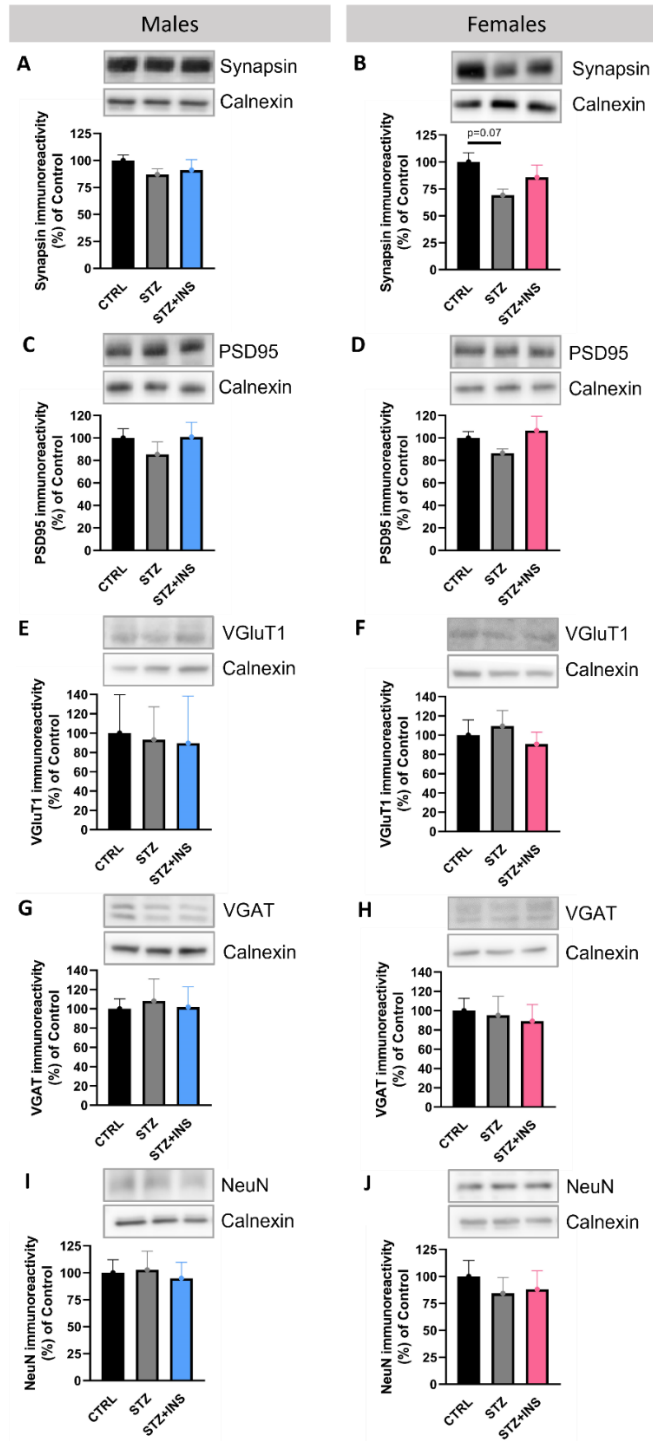


Figure 14: Maternal diabetes does not induce changes retinal synaptic and neuronal protein levels in male and female offspring at P7. On the left are the results concerning retinal protein levels in males with representative images of the blots above the graphs and on the right are the results corresponding to females. We used between 4-8 pups for each group in each sex. **(A,B)** Levels of synapsin, **(C,D)** PSD95 **(E,F)** VGlut1 **(G, H)** VGAT and of **(I, J)** NeuN normalized to control, at P7. Statistical analysis was assessed with ANOVA or Kruskal-Wallis test in data-sets that do not assume a Gaussian distribution.

3.2.2. Maternal diabetes does not induce changes in the number of RGCs in male and female offspring at early infancy

Despite the previous molecular findings, there are evidences that diabetes during pregnancy may reduce the number of RGCs (Najafdari et al., 2014; Singh et al., 2019). Additionally, since during regular development, RGCs undergo a peak period of cell death at early infancy (Sernagor et al., 2001), we aimed to evaluate if maternal diabetes would have an impact on RGCs number at P7 and if so, whether insulin treatment could prevent those changes. For that, the number of Brn3a positive cells in immuno-stained whole-mounted retinas were counted (Figure 15, A, C). No statistically differences were observed between groups (Figure 15, B, D), suggesting that maternal diabetes does not impact RGCs number at offspring retina.

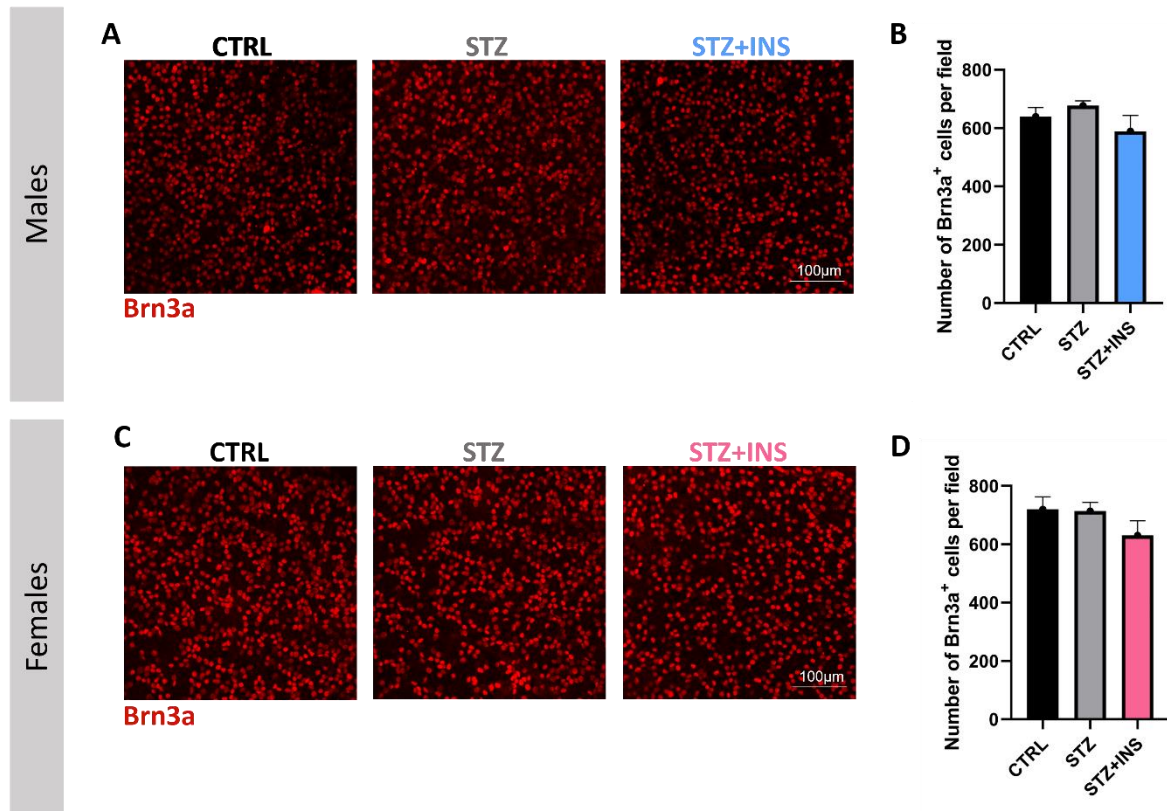


Figure 15: Maternal diabetes does not induce changes in the number of RGCs in male and female offspring at P7. (A) Representative images of male Brn3a immunostained retinas. (B) Number of Brn3a positive cells per field in CTRL, STZ and STZ+INS male offspring. (C) Representative images of female Brn3a immuno-stained retinas. (D) Number of Brn3a positive cells per field in CTRL, STZ and STZ+INS female offspring. Scale bar: 100µm. Values are presented as the mean ± SEM of 4-5 animals. Statistical analysis was assessed with ANOVA or Kruskal-Wallis test in data-sets that do not assume a Gaussian distribution.

3.2.3. Impact of maternal diabetes on microglia number, morphology, and CX3CR1 protein levels at early infancy

Since microglia play a fundamental role in retinal development, namely in regulating the number of newborn neurons and synapses, we investigated if maternal diabetes may induce changes in retinal microglia number and morphology at P7. The number of microglia was counted in Iba-1 stained retinal slices (Figure 16A, B). The number of microglia per retinal layer (GCL+IPL, INL, OPL) and in the total retina was assessed.

In males, the number of microglia on GCL+IPL (Figure 16C) in STZ offspring did not appear different than in CTRL. However, this number was significantly higher in STZ+INS offspring when compared with CTRL ($p=0.0019$) and STZ ($p=0.0026$) (CTRL σ : 4.8 ± 0.4 ; STZ σ : 4.8 ± 0.9 ; STZ+INS σ : 9.2 ± 0.4). In the GCL+IPL of females (Figure 16F) this difference ($p=0.02$) was only detected between CTRL and STZ+INS (CTRL ♀ : 2.9 ± 0.6 ; STZ+INS ♀ : 7.3 ± 0.3).

In the INL of males (Figure 16D), no difference was observed between the number of microglia in STZ and CTRL offspring. It was noticed a tendency ($p=0.054$) for a higher number of microglia in STZ+INS offspring when compared with CTRL (CTRL σ : 2.1 ± 0.3 ; STZ+INS σ : 3.4 ± 0.4). In females (Figure 16G) there were significantly more microglial cells in both STZ ($p=0.01$) and STZ+INS ($p=0.02$) offspring when compared to CTRL (CTRL ♀ : 1.0 ± 0.2 ; STZ ♀ : 2.6 ± 0.3 ; STZ+INS ♀ : 2.4 ± 0.4).

In the OPL (Figure 16E) it was observed a tendency ($p=0.077$) for a lower number of microglia in STZ+INS males when compared to CTRL males (CTRL σ : 0.9 ± 0.2 ; STZ+INS σ : 0.3 ± 0.2).

Regarding the number of microglial cells in the total retina (Figure 16I), there was a higher number of microglia in STZ+INS offspring retina when compared with both CTRL ($p=0.007$) and STZ ($p=0.01$) in males and when compared with CTRL ($p=0.02$) in females (Figure 16K) (CTRL σ : 7.8 ± 0.6 ; STZ σ : 8.0 ± 1.1 ; STZ+INS σ : 12.8 ± 0.8 ; CTRL ♀ : 4.9 ± 0.7 ; STZ+INS ♀ : 10.2 ± 0.3).

Microglia morphology was assessed through manual reconstruction of individual cells in the GCL + IPL layers in retinal wholemounts (Figure 16M, N).

In terms of microglia morphology at P7, a significant difference ($p=0.03$) was found between STZ+INS and CTRL males regarding ramification number on the first branch order (Figure 16, O), being STZ+INS microglia hyper-ramified when compared with CTRL (CTRL σ : $5.1 \pm 0.3 \mu\text{m}$; STZ+INS σ : $6.3 \pm 0.2 \mu\text{m}$). Additionally, a tendency ($p=0.09$) for increased branch length in STZ+INS males' 4th branch order was detected when compared with STZ ones (Figure 16P) (STZ σ : $12.5 \pm 0.9 \mu\text{m}$; STZ+INS σ : $21.3 \pm 3.8 \mu\text{m}$).

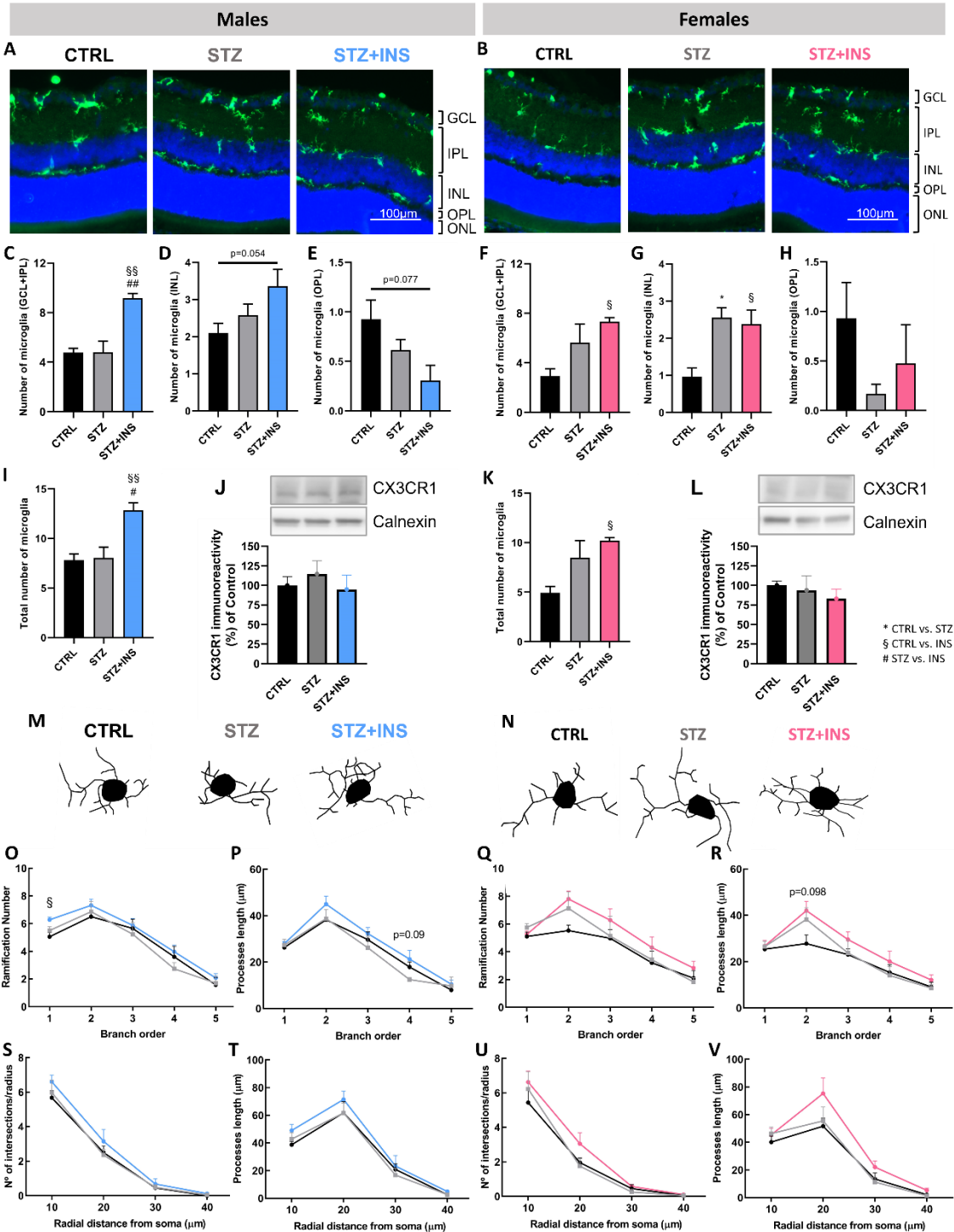


Figure 16: Diabetes during pregnancy does not impact microglia number, morphology and fractalkine receptor levels in the retina at early infancy. (A,B) Representative images of the retina for the three experimental groups (CTRL, STZ and STZ+INS) showing Iba1 stained microglia in green. Males are represented on the left and females on the right side. Scale bar: 100 μm. **(C, D, E, F, G, H, I, K)** Number of microglia per retina layer and in total retina in both males (blue) and females (pink). **(J, L)** CX3CR1 immunoreactivity in males and females, respectively, normalized to CTRL. Representative

Western blot images are above the graphs. **(M, N)** Manual reconstruction of Iba-1 stained microglia from GCL and IPL layers of the retina at P7. The number of ramifications **(O, Q)** and processes length **(P, R)** per branch order and number of processes **(S, U)** and processes length **(T, V)** per radius were compared between CTRL, STZ and STZ+INS in both sexes. The results are presented as mean \pm SEM of 4-5 offspring. Statistical analysis was assessed with ANOVA or Kruskal-Wallis test in data sets that do not assume a Gaussian distribution; * $p < 0.05$: STZ (grey) compared with CTRL (black) offspring; § $p < 0.05$, §§ $p < 0.01$: CTRL compared with STZ+INS (blue and pink) offspring; # $p < 0.05$, ## $p < 0.01$: STZ compared with STZ+INS offspring.

In females, in the STZ+INS group there was a tendency ($p = 0.098$) for an increase in the length of microglia processes of the 2nd order comparing with CTRL (Figure 16R) (CTRL♀: 27.8 ± 3.7 ; STZ+INS♀: 42.0 ± 4.1).

Early infancy is a phase of maturation, synaptic pruning and phagocytosis of neurons, processes in which microglia are strongly involved via fractalkine signaling pathway (Paolicelli et al., 2014). Therefore, fractalkine receptor levels were measured in the offspring retinal total extracts (Figure 16J, L).

No changes were detected regarding CX3CR1 immunoreactivity when comparing CTRL, STZ and STZ+INS groups in both males and females (Figure 16J, L).

3.3. Impact of maternal diabetes on offspring retina at late infancy

3.3.1. Diabetes during pregnancy induces changes in retinal structure

At P21, after eye opening, it is possible to assess retina structure through OCT (Figure 17A, G) in order to detect changes that may be induced by hyperglycemia during gestation. The thickness of the several layers (NFL+GCL+IPL, INL, ONL and IS/OS) and of total retina was assessed in CTRL, STZ and STZ+INS male and female offspring.

In males, no changes were found in total retina thickness and in most layers. However, in IS/OS layer (Figure 17E), the thickness was significantly diminished in STZ offspring when compared with CTRL ($p = 0.02$), an effect prevented by insulin administration to the dam (STZ+INS: $p = 0.04$) (CTRL♂: $41.2 \pm 1.8 \mu\text{m}$; STZ♂: $33.6 \pm 1.8 \mu\text{m}$; STZ+INS♂: $41.7 \pm 2.6 \mu\text{m}$).

STZ females presented a tendency for a thinning of NFL+GCL+IPL (Figure 17H) when compared with CTRL ($p = 0.08$), an effect prevented by insulin dam administration (STZ+INS: $p = 0.01$) (CTRL♀: $69.4 \pm 2.1 \mu\text{m}$; STZ♀: $64.2 \pm 0.9 \mu\text{m}$; STZ+INS♀: $71.6 \pm 0.8 \mu\text{m}$). In IS/OS layer (Figure 17K), a tendency for decreased thickness was found in STZ offspring when compared with CTRL ($p = 0.07$) an effect also prevented by dam insulin treatment (STZ+INS: $p = 0.03$) (CTRL♀: $40.7 \pm 1.6 \mu\text{m}$; STZ♀: $34.4 \pm 1.2 \mu\text{m}$; STZ+INS♀: $42.1 \pm 2.0 \mu\text{m}$). No changes were observed in female total retina thickness.

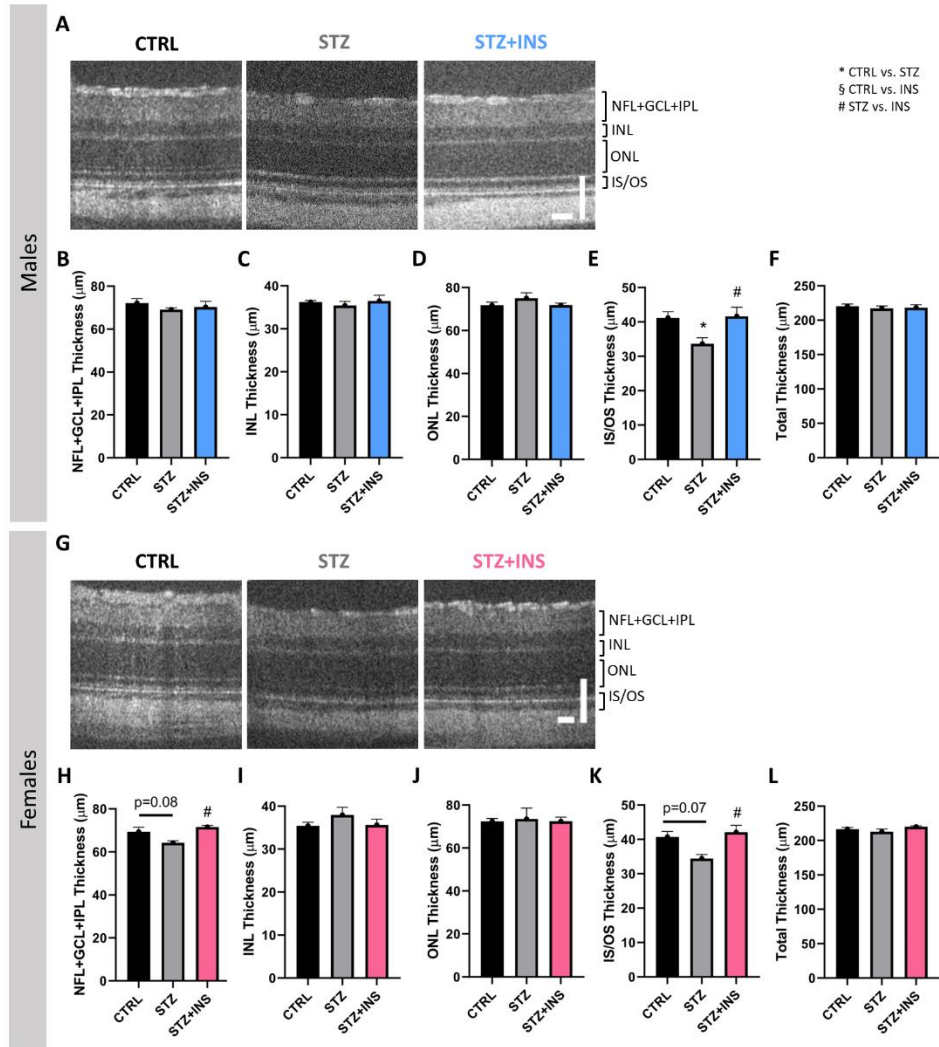


Figure 17: Diabetes during pregnancy induces changes in retina thickness. (A, G) Representative OCT images for CTRL, STZ and STZ+INS males and females' offspring, respectively. Thickness of each retina layer and total retina thickness in males (**B, C, D, E, F**) and females (**H, I, J, K, L**). Results are presented as mean \pm SEM of 4-12 offspring. Statistical analysis was assessed with ANOVA or Kruskal-Wallis test in data sets that do not assume a Gaussian distribution; * $p < 0.05$: STZ (grey) compared with CTRL (black) offspring; # $p < 0.05$: STZ compared with STZ+INS (blue and pink) offspring.

3.3.2. Diabetes during pregnancy induces changes in offspring retinal function

Since maternal diabetes may impact retinal neuronal activity, the electrical response of various neuronal types in the offspring retina was assessed by ERG. We first compared pSTR and nSTR amplitudes in CTRL, STZ and STZ+INS male and female offspring (Figure 18B, C, K, L) and observed no alterations between them.

Then, the scotopic responses were assessed (Figure 18A, J) and a-wave and b-wave amplitudes in CTRL, STZ and STZ+INS offspring were evaluated. In males, significant differences were observed in the a-wave amplitude (Figure 18D, E), for the 3.0 cd·s/m² light stimulus, between STZ and STZ+INS ($p=0.05$; STZ σ : $143.4 \pm 24.9 \mu\text{V}$; STZ+INS σ : $205.5 \pm 28.3 \mu\text{V}$). Regarding b-wave amplitude, a significant difference was found between STZ and STZ+INS ($p=0.03$; STZ σ : $113.8 \pm 17.0 \mu\text{V}$; STZ+INS σ : $194.2 \pm 15.9 \mu\text{V}$), for the 0.03 cd·s/m² light stimulus. With 0.30 cd·s/m² light stimulus, the amplitude of the b-wave was smaller in STZ offspring when compared with CTRL ($p=0.03$), an effect prevented by dam insulin administration (STZ+INS: $p=0.0014$), (CTRL σ : $257.3 \pm 15.9 \mu\text{V}$; STZ σ : $183.4 \pm 29.0 \mu\text{V}$; STZ+INS σ : $297.8 \pm 36.1 \mu\text{V}$). Those differences were also detected with the 0.95 cd·s/m² and 3.00 cd·s/m² light stimulus. With the higher intensity (9.45 cd·s/m²), the differences were only detected between CTRL and STZ ($p=0.008$; CTRL σ : $290.6 \pm 20.7 \mu\text{V}$; STZ σ : $199.6 \pm 15.8 \mu\text{V}$). No changes were found in female retina scotopic responses (Figure 18M, N).

After light adaptation, the photopic ERG was performed and no differences were found in b-wave amplitude between CTRL, STZ and STZ+INS both in male and female offspring retina (Figure 18F, O).

Concerning flicker responses (Figure 18G, P), when comparing the 1st and 2nd harmonic amplitudes, no differences were found in females (Figure 18, Q, R). Nevertheless, in males (Figure 18H, I), with 3.00 cd·s/m² light stimulus, the amplitude of 1st harmonic was smaller in STZ offspring when compared with CTRL ($p=0.036$; CTRL σ : $10.8 \pm 1.5 \mu\text{V}$; STZ σ : $5.7 \pm 1.2 \mu\text{V}$).

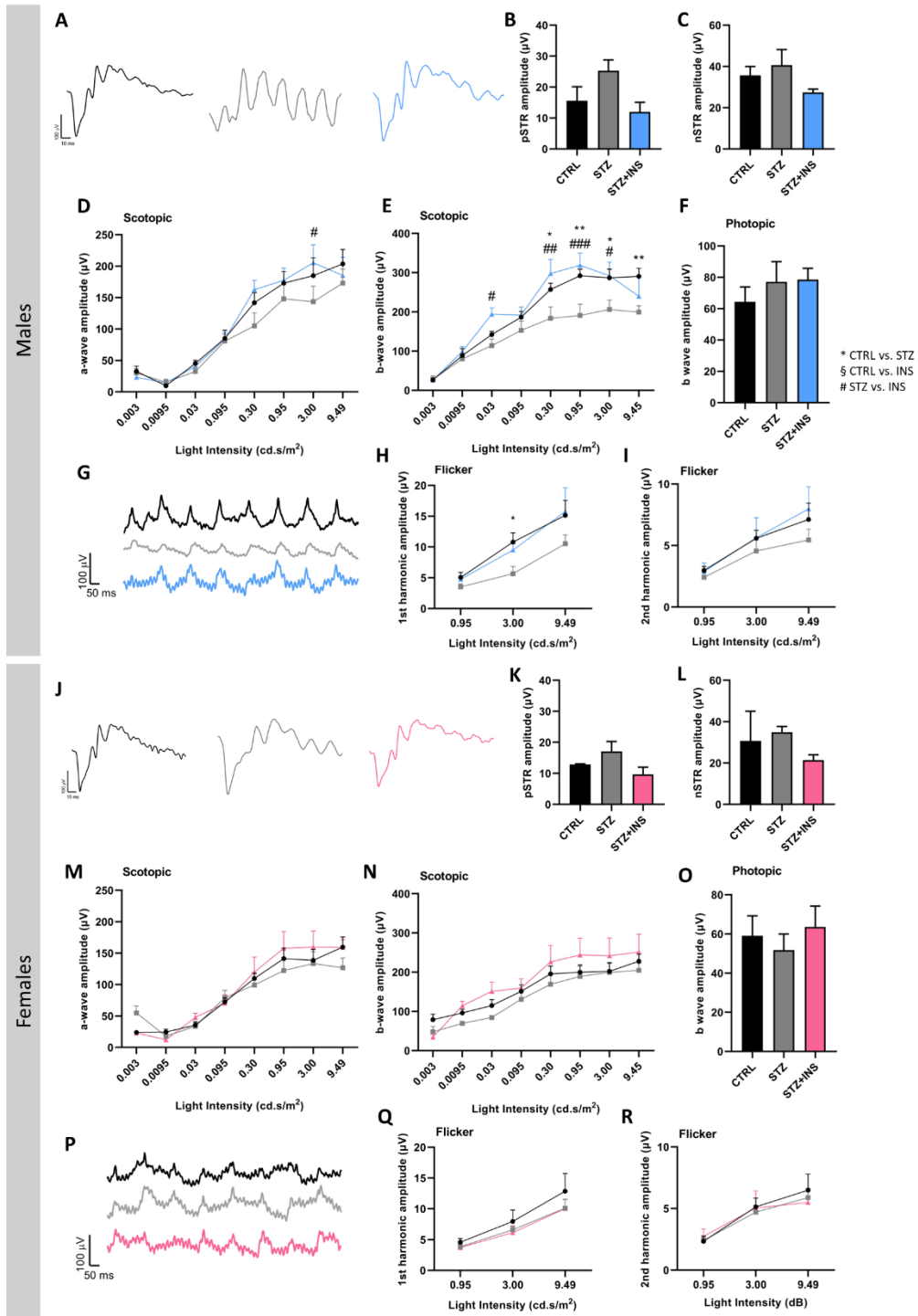


Figure 18: Diabetes during pregnancy induces changes in retinal function. (A, J) Representative images of scotopic response of male and female offspring retina, respectively. **(B, C, K, L)** pSTR and nSTR amplitudes of CTRL, STZ and STZ+INS male and female offspring retina in response to a 0.000095 cd/m^2 light stimulus. **(D, E, M, N)** Scotopic a-wave and b-wave in response to 0.003-9.45 $\text{cd}/\text{s}/\text{m}^2$ light stimulus, in males and females. **(F, O)** Photopic b-wave amplitudes in response to the higher intensity light stimulus (9.49 $\text{cd}/\text{s}/\text{m}^2$). **(G, P)** Representatives of flicker responses in males and females, **(H, I,**

Q, R) 1st and 2nd harmonic amplitudes of the flicker for 0.95-9.49 cd·s/m² light stimulus. Results are presented as mean ± SEM of 3-9 offspring for each group. Statistical analysis was assessed with ANOVA or Kruskal-Wallis test in data-sets that do not assume a Gaussian distribution; *p<0.05, **p<0.01: STZ (grey) compared with CTRL (black) offspring; #p<0.05, ##p<0.01, ###p<0.001: STZ compared with STZ+INS (blue and pink) offspring.

3.3.3. Impact of maternal diabetes on offspring retinal neurons at late infancy

Aiming to associate retinal structural and functional impairments with synaptic or neuronal alterations, we evaluated the protein levels of synapsin, PSD95, VGluT1, VGAT and NeuN in retina total extracts (Figure 19). No significant differences were detected between CTRL, STZ and STZ+INS males or females in any of the proteins evaluated.

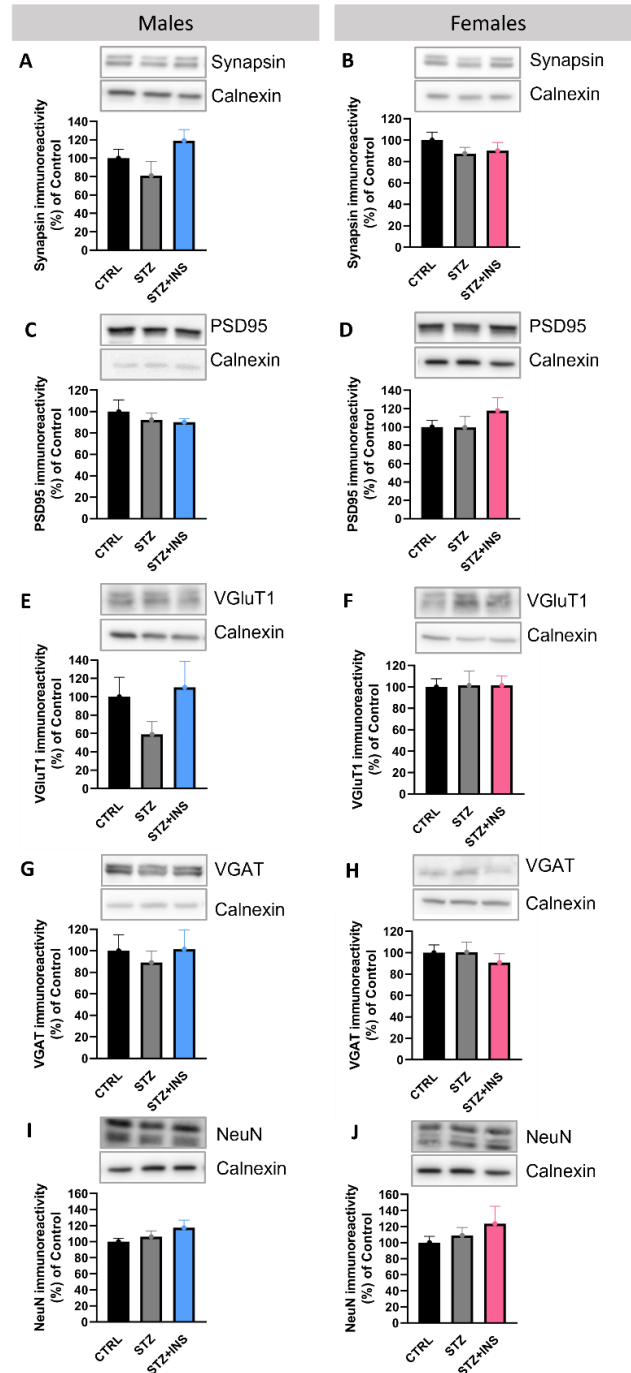


Figure 19: Maternal diabetes does not induce changes in male and female offspring synaptic and neuronal protein levels in the retina at P21. On the left are the results concerning protein levels in males with representative images of Western blots above the graphs and on the right are the results corresponding to females. **(A,B)** Levels of synapsin normalized to control at P21. **(C,D)** Levels of PSD95 normalized to control at P21. **(E,F)** Levels of VGlut1 normalized to control at P21. **(G, H)** Levels of VGAT normalized to control at P21. **(I, J)** Levels of NeuN normalized to control at P21. Results are presented as mean \pm SEM of 5-8 offspring for each group. Statistical analysis was assessed with ANOVA or Kruskal-Wallis test in data sets that do not assume a Gaussian distribution.

3.3.4. Maternal diabetes does not induce changes in the number of RGCs in male and female offspring at late infancy

Although by ERG no differences on the STR (which reflects RGC function) were found, a tendency for a reduction in NFL+GCL+IPL thickness in STZ females was detected. To help us elucidate if RGC number was affected by maternal diabetes, Brn3a positive cells were counted (Figure 20A, C) in retinal wholemounts at P21. No significant alterations were found between groups (Figure 20B, D).

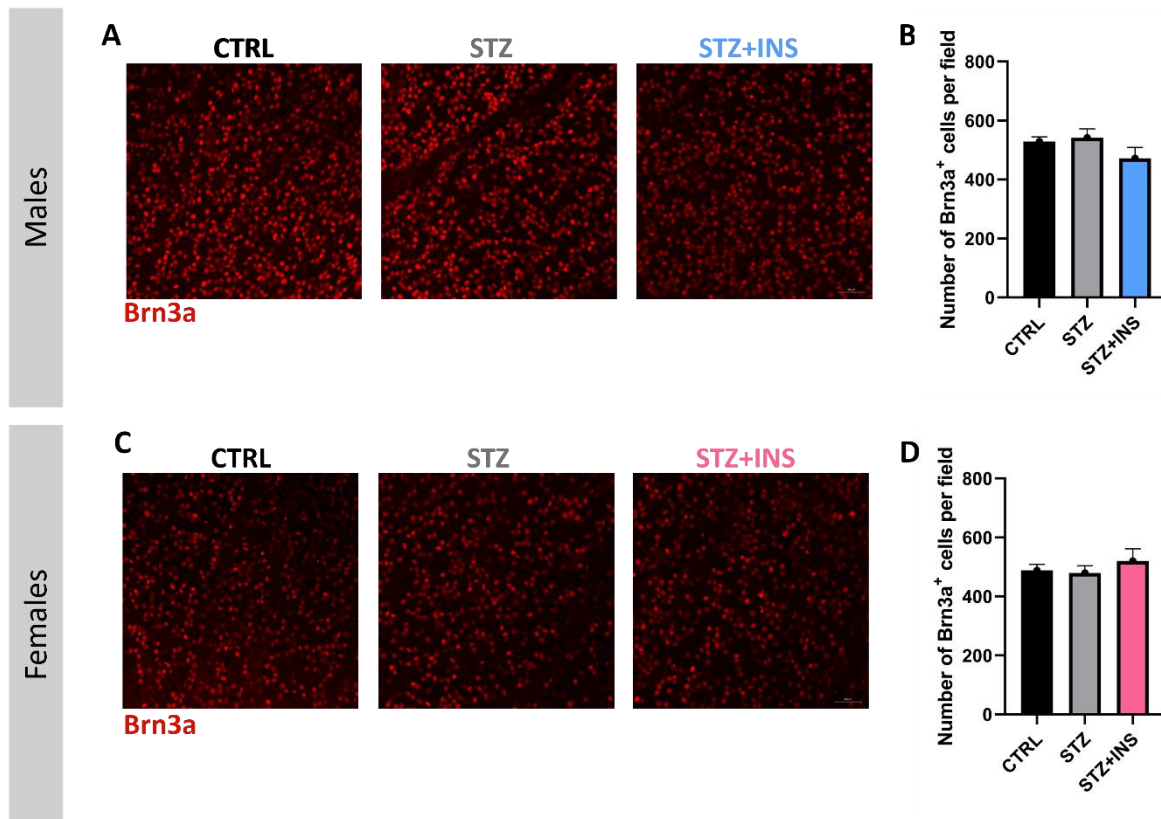


Figure 20: Maternal diabetes does not induce changes in male and female offspring number of RGCs at P21. (A) Representative images of male Brn3a immuno-stained retinas. (B) Number of Brn3a positive cells per field in CTRL, STZ and STZ+INS male offspring. (C) Representative images of female Brn3a immuno-stained retinas. (D) Number of Brn3a positive cells per field in CTRL, STZ and STZ+INS female offspring. Scale bar: 100 μ m. Results are presented as mean \pm SEM of 4-6 offspring. Statistical analysis was assessed with ANOVA or Kruskal-Wallis test in data sets that do not assume a Gaussian distribution.

We observed a decrease in thickness in the IS/OS layer of the offspring retina of diabetic dams. At the same time, in males, changes were detected in cones response (flicker 1st harmonic) and on the scotopic a-wave, which reflects photoreceptors response (Heynen & Van Norren, 1985). Because of these alterations, the levels of arrestin (cone photoreceptor marker) and rhodopsin (rod photoreceptor marker) were evaluated.

In males, no statistically significant alterations in the levels of these proteins were observed. However, in females, a decreased immunoreactivity of arrestin in STZ offspring was found comparing with CTRL (STZ: $p=0.045$), an effect prevented by insulin administration to the diabetic dams (STZ+INS: $p=0.046$) (CTRL♀: 100.0 ± 1.0 ; STZ♀: 64.4 ± 8.9 ; STZ+INS♀: 99.8 ± 10.4).

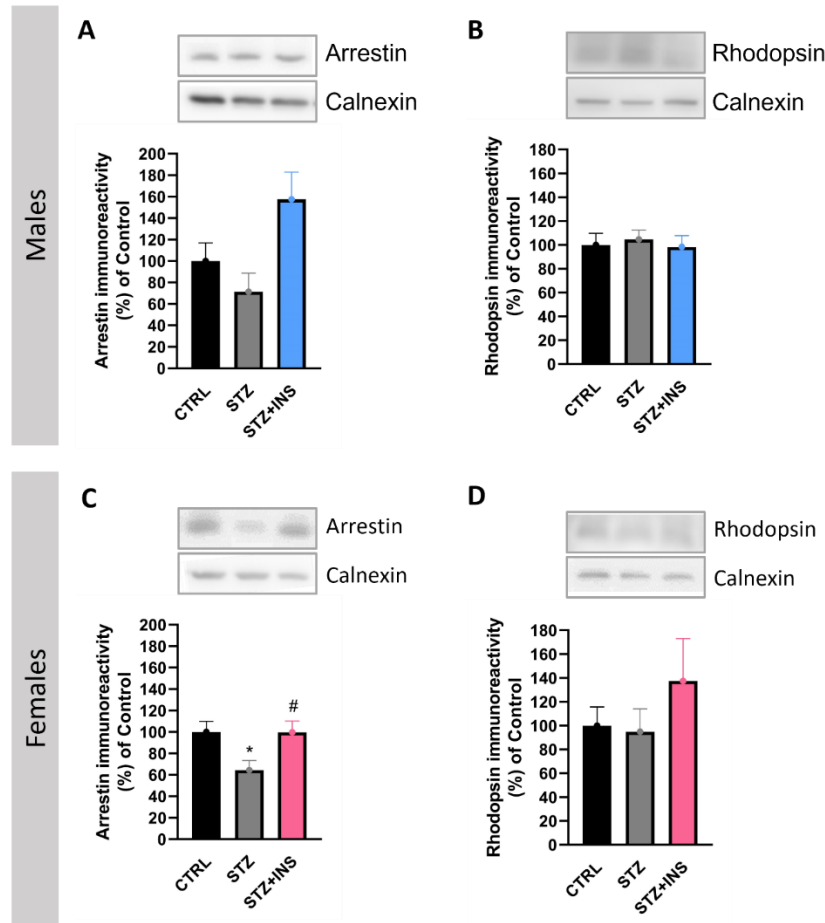


Figure 21: Maternal diabetes induces changes in arrestin levels in females. (A, C) Arrestin immunoreactivity normalized to CTRL in males and females. Representative images of Western blots are presented above the graphs. **(B,D)** Rhodopsin immunoreactivity normalized to CTRL in males and females. Representative images of Western blots are presented above the graphs. Values are presented as the mean \pm SEM of 4–8 animals. Statistical analysis was assessed with ANOVA or Kruskal-Wallis test in data sets that do not assume a Gaussian distribution; * $p<0.05$: STZ (grey) compared with CTRL (black) offspring; # $p<0.05$: STZ compared with STZ+INS (blue and pink) offspring.

3.3.5. Impact of maternal diabetes on microglia number, morphology, and CX3CR1 protein levels at late infancy

Microglial cells are mostly located in the inner retinal layers, presenting ramified cellular processes responsible for immune surveillance (Li et al., 2019). Since diabetes during

pregnancy might induce long-lasting microglial changes, eventually by changing microglia morphology at late infancy, and increasing its proliferation and migration to outer retinal layers, microglia number and morphology were assessed at P21. The number of microglia per layer (GCL+IPL, INL, OPL) and in total retina was counted in Iba-1 stained retinal sections (Figure 22A, B).

No changes were found between CTRL, STZ or STZ+INS in males and females regarding the number of microglia per retinal layer and in total retina (Figure 22C, D, E, F, G, H, I, K).

Microglia morphology was assessed through manual reconstruction of individual cells from GCL and IPL layers in retinal wholemounts (Figure 22M, N).

No changes in microglia morphology were found between CTRL, STZ and STZ+INS males (Figure 22O, P, S, T). On the other hand, in females, although maternal diabetes did not induce changes comparing with the CTRL, significant changes in the number of ramifications per order (between orders 6 and 9) in STZ+INS when compared to CTRL and STZ ($0.001 < p < 0.02$), and a tendency in order 3 ($p=0.055$), 4 ($p=0.09$) and 5 ($p=0.055$) when compared to STZ (Figure 22Q) were found.

In terms of processes length per order (Figure 22R), a significant higher process length was found in STZ+INS microglia in the 9th order when compared to both CTRL ($p=0.005$) and STZ ($p=0.004$) and in the 8th order when compared with CTRL ($p=0.02$). There was also a tendency for increased process length in orders 5 and 6, when compared with STZ ($p=0.07$). Lastly, the number of ramifications that intersect the 10 μm radius was significantly increased in STZ+INS when compared with STZ ($p=0.047$) (Figure 22U).

Regarding CX3CR1 immunoreactivity in retinal total extracts, no changes were detected when comparing CTRL, STZ and STZ+INS groups both in males and females (Figure 22J, L).

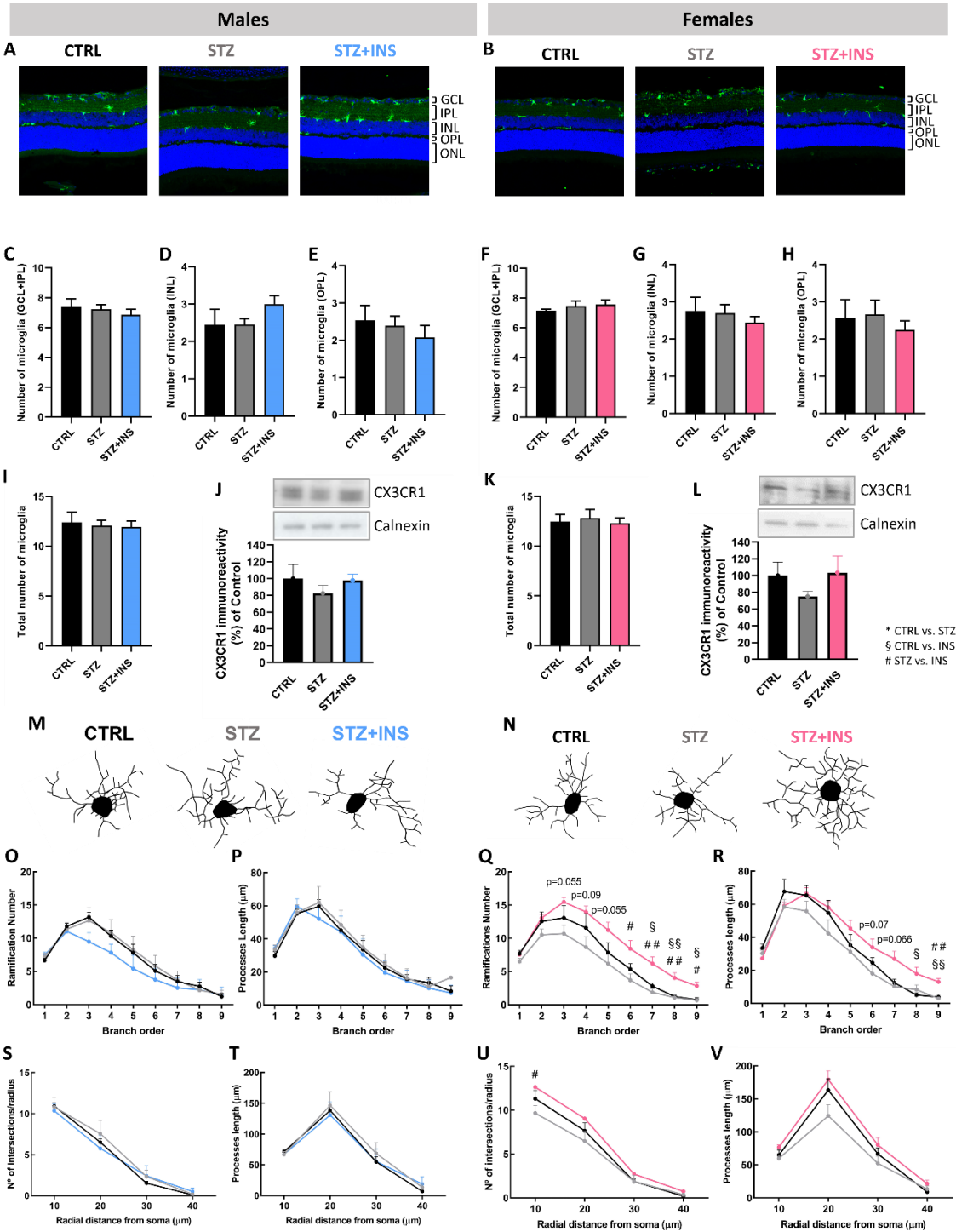


Figure 22: Diabetes during pregnancy does not induce changes in microglia number, morphology and fractalkine receptor levels in late infancy. (A,B) Representative fluorescence images of the retina for the three groups (CTRL, STZ and STZ+INS) showing Iba1 stained microglia in green. Males are represented on the left and females on the right side. Scale bar: 100 µm. **(C, D, E, F, G, H, I, K)** Number of microglia per retina layer and in total retina in both males (blue) and females (pink). For each condition, we used 7-9 offspring. **(J, L)** CX3CR1 immunoreactivity in males and females, normalized to CTRL, using 8 pups for each condition. Representative Western blots are presented

above the graphs. **(M,N)** After manual reconstruction of Iba-1 stained macroglia from the retina (GCL+IPL layers) of males and females at P21, number of ramifications per branch order **(O, Q)**, processes length per branch order **(P, R)**, number of processes per radius **(S, U)** and processes length per radius **(T, V)** were compared between CTRL, STZ and STZ+INS, in both sexes. The results are presented as mean \pm SEM of 4-7 offspring for each condition. Statistical analysis was assessed with ANOVA or Kruskal-Wallis test in data sets that do not assume a Gaussian distribution; §p<0.05, §§p<0.01: STZ+INS (blue and pink) compared with CTRL (black) offspring; #p<0.05, ##p<0.01: STZ (grey) compared with STZ+INS offspring.

Chapter 4: Discussion

4. Discussion

Diabetes during pregnancy has been associated with adverse neonatal outcomes, namely persistent metabolic alterations for the offspring during infancy (Aerts et al., 1990; Dickens & Thomas, 2019; Schwartz & Teramo, 2000; Szmulowicz et al., 2019; Van Assche et al., 2001). Additionally, fetal exposure to hyperglycemia affects the offspring brain, leading to behavioral alterations, memory impairments and increased susceptibility to neurodevelopmental disorders (Kinney et al., 2003; Sousa et al., 2020; Vuong et al., 2017). The offspring's retina, as a part of the CNS, has also been shown to be affected by maternal diabetes, showing some structural and molecular alterations (Najafdari et al., 2014; Singh et al., 2019; Tariq et al., 2010; Titalii-Torres & Morris, 2022). Nevertheless, a comprehensive study of maternal diabetes effects on offspring retinal neurodevelopment, structure and function was missing.

In this work, we hypothesized that maternal diabetes adversely impacts offspring retina development leading to structural and functional deficits, while insulin treatment prevents the changes identified. At the same time, we aimed to clarify if male and female retinas show different vulnerability to hyperglycemia during development, as shown in previous studies on the offspring brain (Kinney et al., 2003; Sousa et al., 2020).

Dams' weight and glycemia were monitored during pregnancy period. Maternal diabetes did not induce alterations in dam weight gain during pregnancy, while presenting hyperglycemia during the entire gestation period. According to the literature, the STZ injection, in the dose used in this study, induces moderate diabetes (Vafaei-Nezhad et al., 2016). However, the values of glycemia presented by the diabetic dams are more in accordance with severe diabetes (Aerts et al., 1990; Kervran et al., 1978).

At P0, we assessed the size of the litters and number of pups of each sex. We observed no significant difference between litter sizes between each experimental group. This is in accordance with what was observed previously (Sousa et al., 2020), showing that maternal diabetes does not influence fetus number or leads to *in utero* fetal death.

While offspring glycemia assessed during the infancy period was unaltered by diabetes during pregnancy, we found that offspring STZ males and females had inferior bodyweight when compared to CTRL at P7 and P21. Insulin administration to the dam was able to completely prevent this change at P7, while only preventing partially at P21. The uncontrolled maternal hyperglycemia induces microsomia and neurodevelopment delay, also described in other studies of severe diabetes (Aerts et al., 1990; Valente Piazza et al., 2019; Van Assche et al., 2001). Initially, maternal hyperglycemia results in fetal early hyperinsulinemia. However, β -cell overstimulation progressively leads to β -cell insulin depletion, resulting in fetal hypoinsulinemia and in a decrease in fetal glucose uptake. Consequently, the growth of fetal protein mass is suppressed inducing offspring microsomia (Van Assche et al., 2001).

Additionally, maternal hyperglycemia disturbs placental nutrient apport, while treatment with insulin may activate placental nutrient transport to the fetus (Araújo et al., 2015; Ruiz-Palacios et al., 2017). In this study, insulin dam administration led to a partial prevention of diabetes effect on offspring's bodyweight at P21. In a previous study, we found that insulin administration prevented macrosomia at P21, and female offspring presented increased bodyweight comparing with controls (Sousa et al., 2020). It is plausible that insulin may bind to receptors present in placenta trophoblast membrane, contributing to placental nutrient metabolism and to fetal development (Hiden et al., 2006; Ruiz-Palacios et al., 2017), resulting in an increase in bodyweight.

Maternal diabetes induced a delay in eye opening day, indicating an impairment on this developmental milestone, and in offspring neurodevelopment. This is in accordance with what we and others have found in previous studies (Sousa et al., 2020; Valente Piazza et al., 2019). On the contrary, mild hyperglycemia was found to induce STZ pups to open the eyes earlier than CTRL ones and to be slightly heavier, though not enough to present macrosomia. In this study of mild GDM, only diabetic dams with glucose levels between 120 and 300 mg/dL at G0 were used for mating (Kiss et al., 2012). In mild hyperglycemia models, the combination of an excess of maternally derived glucose and the consequent fetal hyperinsulinemia stimulates fetal metabolism and may result in fetal and neonatal macrosomia. On the other hand, insulin and other growth factors, such as insulin-like growth factor and epidermal growth factor are prominent determinants of fetal growth and development, which may explain the advance in eye opening (Kiss et al., 2012).

In the present study, dam insulin administration not only prevented the effect of maternal diabetes on offspring eye opening day, but in fact anticipated eye opening day when compared with CTRL offspring, further suggesting that insulin may indeed activate signaling pathways that promote fetal development through insulin receptors present in dam's placenta (Ruiz-Palacios et al., 2017). Similar results were obtained in a previous study using the same animal model (Sousa et al., 2020).

Regarding pup metabolic alterations and eye opening day, STZ male and female offspring were similarly affected, suggesting no sex differences in these parameters.

Impaired neurodevelopment, as the delay in eye opening day suggests, may be mirrored by neuronal and synaptic alterations induced by maternal diabetes. Therefore, the offspring retinas were further evaluated at P7 and P21, corresponding to early and late infancy, respectively, allowing the detection of early changes induced by maternal diabetes. Since this study was focused on the infancy period, the evaluation of sex differences in offspring retinas was carried out without considering the female hormonal fluctuations caused by reproductive hormone cycles (Chaychi et al., 2015; Wood et al., 2001).

At P7, we focused in assessing the impact of maternal diabetes on several proteins suggestive of synaptic or neuronal impairments. No significant changes were detected in the levels of

synaptic/neuronal proteins in STZ males and females, suggesting that maternal diabetes did not compromise retinal synapses and neurons. Nevertheless, in females there was a tendency for lower synapsin-1 (presynaptic marker) levels in STZ offspring when compared with CTRL, an effect not detected in males. This could be suggestive of a decrease in synapse number at early infancy. However, the fact that no changes were found in PSD95, VGlut1 and VGAT protein levels, supports no major changes at glutamatergic and GABAergic synapses. Similar findings were observed at the hippocampus of male and female STZ offspring at P7, further suggesting that maternal diabetes does not impact synapse integrity (Sousa et al., 2020). Additionally, at P7, the protein levels of NeuN, a marker of mature neurons, remained unchanged in the STZ offspring retina, suggesting that neuronal integrity, and also possibly retinal neurogenesis is not affected by maternal diabetes.

Previous studies showed that in offspring of women with T1D, a topless disk (superior nerve fiber loss) occurs more commonly than expected, being the topless disk characterized by an impairment in RGC development in human fetal retinas, possibly due to an exaggerated apoptosis late in the perinatal period (Landau et al., 1998). Despite not having statistically significant differences in NeuN protein levels at P7, we aimed to establish whether at early infancy, a stage of development when RGC undergo reorganization, implying a peak of cell death (Sernagor et al., 2001), maternal diabetes could induce increased RGC loss. We observed no statistically significant differences in RGC number suggesting that maternal diabetes did not induce exaggerated RGC loss. Notably, in previous works on animal models, it was observed that hyperglycemia can reduce the number of RGCs (Najafdari et al., 2014; Singh et al., 2019). Nevertheless, on those studies, different animal models were used. In one case, a rat model of GDM was used, being diabetes induced with 40 mg/kg/body weight of STZ at the first day of gestation (intraperitoneally), and the offspring were evaluated at P28, with no distinction between males and females (Najafdari et al., 2014). In the other study, zebrafish embryos exposed to a high glucose concentration during embryogenesis were evaluated (Singh et al., 2019).

During retina development, microglia is involved in retinal neurogenesis (by microglia-mediated phagocytosis of neurons), synapse refinement and pruning (Li et al., 2019), being microglia morphology and number related with their function (Li et al., 2019). Microglia number was assessed along the retinal layers and their morphology evaluated at the GCL+IPL to assess whether maternal diabetes induces changes in microglia number and morphology in the offspring retina at early infancy. We observed that in both male and female STZ retinas the number of microglia was similar to controls except in female INL, where an increase in the number of microglial cells was detected. Nevertheless, the total number of microglia was similar to CTRL, suggesting that maternal diabetes does not have a considerable impact in microglia number at the offspring retina.

Regarding CX3CR1 immunoreactivity, no changes were detected suggesting that the communication between microglia and neurons may not be affected by maternal diabetes at

P7. Also, maternal diabetes did not induce changes in microglia retinal morphology. In a previous study with a model of GDM induced by high fat and sucrose diet, microglia in the hippocampus appeared to be more amoeboid by E20 in male offspring from diabetic dams, being CX3CR1 levels reduced by 15 weeks of age (Vuong et al., 2017). In the hippocampus of STZ rats we previously found that microglia morphology was similar to CTRL in both males and females (Sousa et al., 2020). Altogether, the fact that CX3CR1 levels, microglia morphology and number were not affected by maternal diabetes, together with no changes in synaptic and neuronal markers, and unchanged number of RGC, further indicates that maternal diabetes does not impact retinal neuronal integrity at early infancy.

Interestingly, insulin administration to the diabetic dam may modulate offspring development differently from what is observed in physiological conditions. It promoted the anticipation of eye opening day, and at early infancy it increased microglia number at male and female GCL+IPL and INL in STZ+INS and in total retina. Similar findings were observed at female hippocampus, where increased number of microglia was found at P7 (Sousa et al., 2020). Nevertheless, at offspring hippocampus, STZ+INS male and female microglia are hyper-ramified comparing to CTRL, an effect not observed at the retina at the same timepoint.

Though molecular and cellular data did not point to impaired retina development at early infancy, eye opening usually occurs between P14 and P17. The delay in eye opening day of STZ offspring suggests possible consequences at later stages of life. Therefore, maternal diabetes impact in retinal structure and function was assessed at late infancy.

By OCT, we observed a thinning of IS/OS layer in STZ males and a tendency to decreased IS/OS and in NFL+GCL+IPL thickness in females, effects prevented by insulin administration to the dams. Interestingly, in zebrafish animal model, it was found that hyperglycemia during embryogenesis induces a decrease in photoreceptor (cones and rods) and horizontal cells number, while not affecting other retinal neurons (Titalii-Torres & Morris, 2022). In fact, at late infancy and similarly to what was observed at early infancy, no changes in the number of RGCs were found in the retinas of both male and female STZ offspring. In contrast, in previous studies, it was reported a reduction in the number of RGCs in models of fetal exposure to hyperglycemia, whereas the thickness of GCL, assessed by histology, was increased (Najafdari et al., 2014; Singh et al., 2019). The authors suggest that this increase in thickness may occur due to inflammation and increased vascular permeability.

The thickness of INL was also increased in zebrafish model, which was associated with activation and hypertrophy of the Müller cells, while IPL, consisting of the synapses formed by the dendrites of the ganglion cells and the axons of the bipolar cells presented decreased thickness, suggesting some degree of synaptic loss (Singh et al., 2019).

Another interesting finding while performing OCTs was that STZ offspring showed increased opacity in the cornea when compared with CTRL, in some cases making OCT acquisition impossible. From the total number of analyzed animals, no CTRL or STZ+INS offspring showed

increased opacity to the point where it would be impossible to perform the OCT, while 48% of STZ offspring had this condition, corresponding to 47% of the males and 50% of the females (data not shown). This cataract-like alteration in STZ offspring was also reported in previous studies (Giavini & Prati, 1990; Simán et al., 2009).

Additionally, we performed ERGs to assess any signs of retinal neuronal dysfunction, namely photoreceptor, bipolar cells and RGCs dysfunction. In the case of RGCs, which activity is reflected by STR response, we observed that maternal diabetes does not induce changes in the amplitude, suggesting RGC normal function in male and female STZ retinas.

After analysis of the amplitude of the scotopic a-wave, which is considered to be mainly generated by photoreceptors (Heynen & Van Norren, 1985), we found that maternal diabetes did not induce significant changes in photoreceptor function both in male and female retinas in dark adapted conditions. Nevertheless, by Flicker analysis we were able to assess whether cones were particularly affected since the 1st harmonic reflects cone response (Falsini et al., 1995; Frishman, 2006). We observed that, in males, flicker's 1st harmonic amplitude was smaller in STZ offspring when compared with CTRL showing that cones are affected by maternal diabetes. This effect was prevented by insulin administration to the diabetic dams and was only observed in STZ males and not in females.

Interestingly, when we assessed arrestin and rhodopsin levels to help clarifying these last results, we found decreased levels of arrestin in STZ female offspring retina (which were prevented by insulin administration) whereas the ERGs revealed no alteration in cone response. In contrast we found no significant changes in arrestin levels in male STZ retinas. ERG analysis and molecular data suggest that maternal diabetes may impact cone photoreceptors, being these neurons particularly vulnerable to maternal hyperglycemia during development.

Notably, studies in zebrafish support our findings that photoreceptors are susceptible for damage, since hyperglycemia during embryogenesis induced a decrease in photoreceptors number. The authors suggested that hyperglycemia may induce a delay in photoreceptor differentiation or cell death (Titalii-Torres & Morris, 2022).

Regarding bipolar cell function, maternal diabetes also induced a decrease in the scotopic b-wave amplitudes in STZ males (though in photopic conditions no changes were detected), meaning that bipolar cells may also be dysfunctional in STZ offspring scotopic pathway. This effect was prevented by insulin administration to the diabetic dams, and only observed in males, putting forward the possibility that male offspring retinal neurons to be more vulnerable to hyperglycemia and suggesting some sex-related resilience of female retinas.

Aiming to further associate retinal structural and functional changes induced by maternal diabetes, with possible long-lasting changes occurring at synaptic level we further assessed the levels of synaptic proteins in the offspring retina at P21. No changes were found in retinal total extracts. Nevertheless, in future studies it could be important to analyze synaptic

protein immunoreactivity in retinal slices or in retinal synaptosomes since changes may be occurring specifically at synaptic terminal level.

Maternal diabetes also did not induce changes on microglia number, morphology, and fractalkine receptor levels at late infancy, suggesting that maternal diabetes does not affect microglial cells or influence the crosstalk between neuron and microglia that could contribute to synaptic changes and structural and functional alterations. Notably, STZ+INS female microglia were hyper-ramified comparing to CTRL and STZ ones, an effect not observed in males. Notably, we found similar results in the STZ+INS female hippocampus at P21, while in male hippocampus a hyper-ramification of these cells was also found. We hypothesize that this hyper-ramification may be due to a microglia specific insulin response, though the mechanisms underlying it remain to be explored.

Also in the offspring hippocampus, decreased levels of CX3CR1 were found in STZ males. This was accompanied by a tendency to decreased levels of NeuN and VGlut-1 specifically in male STZ offspring hippocampus suggesting a different vulnerability to maternal diabetes between males and females. In the STZ offspring retina, no changes were found in the aforementioned proteins. However, both neuronal tissues appear to be vulnerable to hyperglycemia during development with impact in retinal structure, function, offspring neurodevelopment and behavior at late infancy, which may have long-lasting effects at adulthood. This work puts forward the importance of retinal evaluation of the children exposed to maternal diabetes at infancy and adulthood.

Chapter 5: Conclusions

5. Conclusions

Maternal diabetes is well established to negatively impact the brain of the offspring, giving rise to short- and long- term adverse effects. However, in the retina, which is part of CNS and is considered an extension of the brain, very little was known about the impact of fetal exposure to hyperglycemia on the retina. We hypothesized that diabetes during pregnancy adversely impacts on retina offspring development, leading to structural and functional deficits, and aimed to uncover the possible cellular and molecular changes underpinning such impairments during infancy period. Additionally, we aimed to clarify if diabetes had a sex-specific impact on the retina, as it does on the brain, and whether the treatment of the dam with insulin is able to prevent any changes detected.

Based on the results obtained, we were able to conclude, that:

1. Both male and female offspring of diabetic dams were microsome during evaluation period, being insulin treatment able to partially prevent this, whereas glycemic values were maintained similar to controls.
2. Maternal diabetes induced a delay in eye opening day, a fundamental developmental milestone, in both male and female offspring. Insulin treatment of the diabetic dams anticipated eye opening day comparing to physiological conditions.
3. The levels of synaptic proteins were not altered in male and female offspring of diabetic dams and no major changes were detected in microglial cells suggesting that maternal diabetes does not have a major impact in synaptic integrity during infancy.
4. At P21, maternal diabetes induced a reduction in retina IS/OS layer thickness in both males and females, induced cone dysfunction in males and decreased the levels of cone arrestin in females, effects prevented by insulin administration, thus suggesting that photoreceptors are particularly vulnerable to hyperglycemia.
5. A reduction in NFL+GCL+IPL layers thickness was found only in females, but this was unrelated with a decrease in RGC number, since no RGC loss was found.
6. Maternal diabetes also negatively impacted male offspring bipolar cell's function, being insulin treatment able to prevent this effect.

Summing up, the exposure to hyperglycemia during gestation has indeed an impact in retina development which can, in most cases, be prevented by insulin. At the same time, diabetes controlled by insulin administration may also cause distinct alterations on the offspring retina that differ from what is observed in control conditions. Furthermore, each sex shows different vulnerabilities at different time-points, reinforcing the fact that diabetes induces changes in

the CNS of both sexes in a sex-specific way. Both the brain and the retina present vulnerabilities to diabetes during pregnancy that may be tissue specific.

This work provided some insight that was missing about the impact of maternal diabetes in the developing retina and may inspire future developments in this topic that can help elucidating the mechanisms behind the observed alterations. In the long run, it may open a door to preventive treatments that change the path of comorbidities development in descents of diabetic mothers in a sex specific way.

References

- Aerts, L., Holemans, K., & Van Assche, F. A. (1990). Maternal diabetes during pregnancy: Consequences for the offspring. *Diabetes/Metabolism Reviews*, *6*(3), 147–167. <https://doi.org/10.1002/dmr.5610060303>
- Araújo, J. R., Keating, E., & Martel, F. (2015). Impact of Gestational Diabetes Mellitus in the Maternal-to-Fetal Transport of Nutrients. *Current Diabetes Reports*, *15*(2). <https://doi.org/10.1007/s11892-014-0569-y>
- Berger, A., Cavallero, S., Dominguez, E., Barbe, P., Simonutti, M., & J, S. (2014). Spectral-domain optical coherence tomography of the rodent eye: Highlighting layers of the outer retina using signal averaging and comparison with histology. *PLOS ONE*, *9*(5). <https://doi.org/10.1371/journal.pone.0096494>
- Bloomfield, S. A., & Dacheux, R. F. (2001). Rod vision: Pathways and processing in the mammalian retina. *Progress in Retinal and Eye Research*, *20*(3), 351–384. [https://doi.org/10.1016/S1350-9462\(00\)00031-8](https://doi.org/10.1016/S1350-9462(00)00031-8)
- Brandli, A., & Stone, J. (2015). Using the Electroretinogram to Assess Function in the Rodent Retina and the Protective Effects of Remote Limb Ischemic Preconditioning. *Journal of Visualized Experiments*, *100*. <https://doi.org/10.3791/52658>
- Brown, B. M., Ramirez, T., Rife, L., & Craft, C. M. (2010). Visual Arrestin 1 Contributes to Cone Photoreceptor Survival and Light Adaptation. *Invest Ophthalmol Vis Sci*, *51*, 2372–2380. <https://doi.org/10.1167/iovs.09-4895>
- Bui, B. V, He, Z., Vingrys, A. J., Nguyen, C. T. O., Wong, V. H. Y., & Fortune, B. (2013). Using the Electroretinogram to Understand How Intraocular Pressure Elevation Affects the Rat Retina. *Journal of Ophthalmology*, *2013*, 15. <https://doi.org/10.1155/2013/262467>
- Chaychi, S., Polosa, A., Lachapelle, P., & Barnes, S. (2015). Differences in Retinal Structure and Function between Aging Male and Female Sprague-Dawley Rats are Strongly Influenced by the Estrus Cycle. *PLoS ONE*, *10*(8). <https://doi.org/10.1371/journal.pone.0136056>
- Checchin, D., Sennlaub, F., Levavasseur, E., Leduc, M., & Chemtob, S. (2006). Potential role of microglia in retinal blood vessel formation. *Investigative Ophthalmology and Visual Science*, *47*(8), 3595–3602. <https://doi.org/10.1167/iovs.05-1522>
- Collin, S. P. (2008). A web-based archive for topographic maps of retinal cell distribution in vertebrates: Invited Paper. *Clinical and Experimental Optometry*, *91*(1), 85–95. <https://doi.org/10.1111/j.1444-0938.2007.00228.x>
- Deming, J. D., Pak, J. S., Brown, B. M., Kim, M. K., Aung, M. H., Eom, Y. S., Shin, J. A., Lee, E. J., Pardue, M. T., & Craft, C. M. (2015). Visual cone arrestin 4 contributes to visual function and cone health. *Investigative Ophthalmology and Visual Science*, *56*(9), 5407–5416. <https://doi.org/10.1167/iovs.15-16647>

- Dickens, L. T., & Thomas, C. C. (2019). Updates in Gestational Diabetes Prevalence, Treatment, and Health Policy. *Current Diabetes Reports*, 19(6).
<https://doi.org/10.1007/S11892-019-1147-0>
- Dionne, G., Boivin, M., Séguin, J. R., Pérusse, D., & Tremblay, R. E. (2008). Gestational diabetes hinders language development in offspring. *Pediatrics*, 122(5).
<https://doi.org/10.1542/peds.2007-3028>
- Falsini, B., Porciatti, V., Fadda, A., Merendino, E., Iarossi, G., & Cermola, S. (1995). The first and second harmonics of the macular flicker electroretinogram: Differential effects of retinal diseases. *Documenta Ophthalmologica*, 90(2), 157–167.
<https://doi.org/10.1007/BF01203335>
- Famiglietti Jr, E. V., & Kolb, H. (1976). Structural Basis for ON- and OFF-Center Responses in Retinal Ganglion Cells. *Science*, 194(4261), 193–195.
<https://doi.org/10.1126/science.959847>
- Fan, W. J., Li, X., Yao, H. L., Deng, J. X., Liu, H. L., Cui, Z. J., Wang, Q., Wu, P., & Deng, J. B. (2016). Neural differentiation and synaptogenesis in retinal development. *Neural Regeneration Research*, 11(2), 312–318. <https://doi.org/10.4103/1673-5374.177743>
- Ferrara, A. (2007). Increasing Prevalence of Gestational Diabetes Mellitus. *Diabetes Care*, 30(2), S141–S146. <https://doi.org/10.2337/dc07-s206>
- Field, G. D., & Chichilnisky, E. J. (2007). Information processing in the primate retina: Circuitry and coding. *Annual Review of Neuroscience*, 30, 1–30.
<https://doi.org/10.1146/annurev.neuro.30.051606.094252>
- Fletcher, T. L., Cameron, P., De Camilli, P., & Banker, G. (1991). The Distribution of Synapsin I and Synaptophysin in Hippocampal Neurons Developing in Culture. *The Journal of Neuroscience*, 11(6), 1617–1626. <https://doi.org/10.1523/JNEUROSCI.11-06-01617.1991>
- Fraser, A., Nelson, S. M., MacDonald-Wallis, C., & Lawlor, D. A. (2012). Associations of existing diabetes, gestational diabetes, and glycosuria with offspring iq and educational attainment: The avon longitudinal study of parents and children. *Experimental Diabetes Research*, 2012. <https://doi.org/10.1155/2012/963735>
- Frishman, L. J. (2006). Origins of the Electroretinogram. In J. R. Heckenlively & G. B. Arden (Eds.), *Principles and practice of clinical electrophysiology of vision* (2nd ed., pp. 139–183). <https://doi.org/https://doi.org/10.7551/mitpress/5557.001.0001>
- Frost, J. L., & Schafer, D. P. (2016). Microglia: Architects of the Developing Nervous System. *Trends in Cell Biology*, 26(8), 587–597. <https://doi.org/10.1016/j.tcb.2016.02.006>
- Garner, C. C., Zhai, R. G., Gundelfinger, E. D., & Ziv, N. E. (2002). Molecular mechanisms of CNS synaptogenesis. *Trends in Neurosciences*, 25(5), 243–250.
[https://doi.org/10.1016/S0166-2236\(02\)02152-5](https://doi.org/10.1016/S0166-2236(02)02152-5)

- Giavini, E., & Prati, M. (1990). Morphogenesis of diabetes-induced congenital cataract in the rat. *Acta Anatomica*, *137*(2), 132–136. <https://doi.org/10.1159/000146872>
- Heynen, H., & Van Norren, D. (1985). Origin of the electroretinogram in the intact macaque eye-I. Principal component analysis. *Vision Research*, *25*(5), 697–707. [https://doi.org/10.1016/0042-6989\(85\)90176-2](https://doi.org/10.1016/0042-6989(85)90176-2)
- Hidden, U., Maier, A., Bilban, M., Ghaffari-Tabrizi, N., Wadsack, C., Lang, I., Dohr, G., & Desoye, G. (2006). Insulin control of placental gene expression shifts from mother to foetus over the course of pregnancy. *Diabetologia*, *49*(1), 123–131. <https://doi.org/10.1007/S00125-005-0054-X>
- Huang, D., Swanson, E. a, Lin, C. P., Schuman, J. S., Stinson, W. G., Chang, W., Hee, M. R., Flotire, T., Gregory, K., Puliafito, C. a, & Fujimoto, J. G. (1991). Optical Coherence Tomography. *Science*, *254*(5035), 1178–1181. <https://doi.org/10.1126/science.1957169>
- Johns, E. C., Denison, F. C., Norman, J. E., & Reynolds, R. M. (2018). Gestational Diabetes Mellitus: Mechanisms, Treatment, and Complications. *Trends in Endocrinology and Metabolism*, *29*(11), 743–754. <https://doi.org/10.1016/j.tem.2018.09.004>
- Kervran, A., Guillaume, M., & Jost, A. (1978). The Endocrine Pancreas of the Fetus from Diabetic Pregnant Rat. *Diabetologia*, *15*, 387–393. <https://doi.org/10.1007/BF01219648>
- Kharroubi, A. T. (2015). Diabetes mellitus: The epidemic of the century. *World Journal of Diabetes*, *6*(6), 850. <https://doi.org/10.4239/wjd.v6.i6.850>
- Kinney, B. A., Rabe, M. B., Jensen, R. A., & Steger, R. W. (2003). Maternal hyperglycemia leads to gender-dependent deficits in learning and memory in offspring. *Experimental Biology and Medicine*, *228*(2), 152–159. <https://doi.org/10.1177/153537020322800204>
- Kiss, A. C. I., Woodside, B., Felício, L. F., Anselmo-Franci, J., & Damasceno, D. C. (2012). Impact of maternal mild hyperglycemia on maternal care and offspring development and behavior of Wistar rats. *Physiology and Behavior*, *107*(3), 292–300. <https://doi.org/10.1016/j.physbeh.2012.08.001>
- Landau, K., Bajka, J. D., Kirchscla, B. M., Cience, E. L. S., & Ll, I. N. C. A. (1998). Topless Optic Disks in Children of Mothers With Type I Diabetes Mellitus. *American Journal of Ophthalmology*, *9394*(98), 605–611. [https://doi.org/10.1016/s0002-9394\(98\)00016-6](https://doi.org/10.1016/s0002-9394(98)00016-6)
- Li, F., Jiang, D., & Samuel, M. A. (2019). Microglia in the developing retina. *Neural Development*, *14*(1), 1–13. <https://doi.org/10.1186/s13064-019-0137-x>
- Lobov, I. B., Rao, S., Carroll, T. J., Vallance, J. E., Ito, M., Ondr, J. K., Kurup, S., Glass, D. A., Patel, M. S., Shu, W., Morrissey, E. E., McMahon, A. P., Karsenty, G., & Lang, R. A. (2005). WNT7b mediates macrophage-induced programmed cell death in patterning of the vasculature. *Nature*, *437*, 417–421. <https://doi.org/10.1038/nature03928>

- Massey, S. C., Redburn, D. A., & Crawford, M. L. J. (1983). The effects of 2-amino-4-phosphonobutyric acid (APB) on the ERG and ganglion cell discharge of rabbit retina. *Vision Research*, 23(12), 1607–1613. [https://doi.org/10.1016/0042-6989\(83\)90174-8](https://doi.org/10.1016/0042-6989(83)90174-8)
- Morgan, J. L., Schubert, T., & Wong, R. O. (2008). Developmental patterning of glutamatergic synapses onto retinal ganglion cells. *Neural Development*, 3(8). <https://doi.org/10.1186/1749-8104-3-8>
- Nahum Sacks, K., Friger, M., Shoham-Vardi, I., Abokaf, H., Spiegel, E., Sergienko, R., Landau, D., & Sheiner, E. (2016). Prenatal exposure to gestational diabetes mellitus as an independent risk factor for long-term neuropsychiatric morbidity of the offspring. *American Journal of Obstetrics and Gynecology*, 215(3). <https://doi.org/10.1016/j.ajog.2016.03.030>
- Najafdari, S., Rezaei, N., Shafaroodi, M. M., Ghafari, S., & Golalipour, M. J. (2014). Ganglionic Cells Apoptosis in Retinal Layer of Rat Offspring due to Gestational Diabetes. *International Journal of Morphology*, 32(4), 1131–1135. <https://doi.org/10.4067/s0717-95022014000400001>
- Nelson, R., & Kolb, H. (1995). Bipolar Cell Pathways in the Vertebrate Retina. *Webvision: The Organization of the Retina and Visual System [Internet]*. <https://doi.org/PMID:21413382>
- Paolicelli, R. C., Bisht, K., & Tremblay, M. È. (2014). Fractalkine regulation of microglial physiology and consequences on the brain and behavior. *Frontiers in Cellular Neuroscience*, 8(129), 1–10. <https://doi.org/10.3389/fncel.2014.00129>
- Perlman, I. (1983). Relationship between the amplitudes of the b wave and the a wave as a useful index for evaluating the electroretinogram. *British Journal of Ophthalmology*, 67(7), 443–448. <https://doi.org/10.1136/bjo.67.7.443>
- Puñal Id, V. M., Paisley Id, C. E., Brecha Id, F. S., Lee, M. A., Perelli, R. M., Wangid, J., O’koren, E. G., Ackley, C. R., Saban, D. R., Reese, B. E., & Kayid, J. N. (2019). Large-scale death of retinal astrocytes during normal development is non-apoptotic and implemented by microglia. *PLOS Biology*. <https://doi.org/10.1371/journal.pbio.3000492>
- Ramanathan, M., Jaiswal, A. K., & Bhattacharya, S. K. (2000). Hyperglycaemia in pregnancy: Effects on the offspring behaviour with special reference to anxiety paradigms. *Indian Journal of Experimental Biology*, 38(3), 231–236. <https://doi.org/PMID:10927864>
- Reese, B. E. (2011). Development of the retina and optic pathway. *Vision Res*, 51(7), 613–632. <https://doi.org/10.1016/j.visres.2010.07.010>
- Rosolen, S. G., Kolomiets, B., Varela, O., & Picaud, S. (2008). Retinal electrophysiology for toxicology studies: Applications and limits of ERG in animals and ex vivo recordings. *Experimental and Toxicologic Pathology*, 60(1), 17–32. <https://doi.org/10.1016/j.etp.2007.11.012>

- Ruiz-Palacios, M., Ruiz-Alcaraz, A. J., Sanchez-Campillo, M., & Larqué, E. (2017). E-Mail Role of Insulin in Placental Transport of Nutrients in Gestational Diabetes Mellitus. *Annals of Nutrition & Metabolism*, *70*, 16–25. <https://doi.org/10.1159/000455904>
- Sadeghi, A., Esfandiary, E., Hami, J., Khanahmad, H., Hejazi, Z., Mardani, M., & Razavi, S. (2018). The effects of maternal diabetes and insulin treatment on neurogenesis in the developing hippocampus of male rats. *Journal of Chemical Neuroanatomy*, *91*, 27–34. <https://doi.org/10.1016/j.jchemneu.2018.03.005>
- Santos, Ana M., Calvente, R., Tassi, M., Carrasco, M.-C., Martín-Oliva, D., Marín-Teva, J. L., Navascués, J., & Cuadros, M. A. (2008). Embryonic and Postnatal Development of Microglial Cells in the Mouse Retina. *The Journal of Comparative Neurology*, *506*, 224–239. <https://doi.org/10.1002/cne.21538>
- Schuster, D. P., & Duvuuri, V. (2002). Diabetes mellitus. *Clinics in Podiatric Medicine and Surgery*, *19*(1), 79–107. [https://doi.org/10.1016/S0891-8422\(03\)00082-X](https://doi.org/10.1016/S0891-8422(03)00082-X)
- Schwartz, R., & Teramo, K. A. (2000). Effects of Diabetic Pregnancy on the Fetus and Newborn Metabolic Effects of Maternal Diabetes in the Fetus and the Newborn Infant. *Seminars in Perinatology*, *24*(2), 120–135. <https://doi.org/10.1053/sp.2000>.
- Sernagor, E., Eglén, S. J., & Wong, R. O. L. (2001). Development of Retinal Ganglion Cell Structure and Function. *Progress in Retinal and Eye Research*, *20*(2), 139–174. [https://doi.org/10.1016/S1350-9462\(00\)00024-0](https://doi.org/10.1016/S1350-9462(00)00024-0)
- Sheng, M., & Hoogenraad, C. C. (2007). The Postsynaptic Architecture of Excitatory Synapses: A More Quantitative View. *Annual Review of Biochemistry*, *76*, 823–847. <https://doi.org/10.1146/annurev.biochem.76.060805.160029>
- Sieving, P. A., Murayama, K., & Naarendorp, F. (1994). Push-pull model of the primate photopic electroretinogram: A role for hyperpolarizing neurons in shaping the b-wave. *Visual Neuroscience*, *11*(3), 519–532. <https://doi.org/10.1017/S0952523800002431>
- Simán, C. M., Naeser, P., & Eriksson, U. J. (2009). Increased lenticular aldose reductase activity and high incidence of congenital cataract in the offspring of diabetic rats. *Acta Ophthalmologica*, *71*(5), 629–636. <https://doi.org/doi:10.1111/j.1755-3768.1993.tb04652.x>
- Singh, A., Castillo, H. A., Brown, J., Kaslin, J., Dwyer, K. M., & Gibert, Y. (2019). High glucose levels affect retinal patterning during zebrafish embryogenesis. *Nature*, *9*(4121). <https://doi.org/10.1038/s41598-019-41009-3>
- Sousa, F. J., Correia, R. G., Cruz, A. F., Martins, J. M., Rodrigues, M. S., Gomes, C. A., Ambrósio, A. F., & Baptista, F. I. (2020). Sex differences in offspring neurodevelopment, cognitive performance and microglia morphology associated with maternal diabetes: Putative targets for insulin therapy. *Brain, Behavior, & Immunity - Health*, *5*(100075). <https://doi.org/10.1016/j.bbih.2020.100075>
- Szmulowicz, E. D., Josefson, J. L., & Metzger, B. E. (2019). Gestational Diabetes Mellitus.

Endocrinology and Metabolism Clinics of North America, 48(3), 479–493.
<https://doi.org/10.1016/j.ecl.2019.05.001>

- Tabasi, A., Ghafari, S., Mehdizadeh, M., Shekari, M. A., & Golalipour, M. J. (2017). Gestational diabetes influences retinal Muller cells in rat's offspring. *Iran J Basic Med Sci*, 20, 216–221. <https://doi.org/10.22038/ijbms.2017.8251>
- Tariq, Y. M., Samarawickrama, C., Li, H., Huynh, S. C., Burlutsky, G., & Mitchell, P. (2010). Retinal thickness in the offspring of diabetic pregnancies. *American Journal of Ophthalmology*, 150(6), 883–887. <https://doi.org/10.1016/j.ajo.2010.06.036>
- Telegina, D. V., Kozhevnikova, O. S., Antonenko, A. K., & Kolosova, N. G. (2021). Features of retinal neurogenesis as a key factor of age-related neurodegeneration: Myth or reality? *International Journal of Molecular Sciences*, 22(14). <https://doi.org/10.3390/ijms22147373>
- Tian, N. (2004). Visual experience and maturation of retinal synaptic pathways. *Vision Research*, 44(28), 3307–3316. <https://doi.org/10.1016/j.visres.2004.07.041>
- Titalii-Torres, K. F., & Morris, A. C. (2022). Embryonic hyperglycemia perturbs the development of specific retinal cell types, including photoreceptors. *Journal of Cell Science*, 135(1). <https://doi.org/10.1242/jcs.259187>
- Vafaei-Nezhad, S., Hami, J., Sadeghi, A., Ghaemi, K., Hosseini, M., Abedini, M. R., & Haghir, H. (2016). The impacts of diabetes in pregnancy on hippocampal synaptogenesis in rat neonates. *Neuroscience*, 318, 122–133. <https://doi.org/10.1016/J.NEUROSCIENCE.2016.01.025>
- Valente Piazza, F., Segabinazi, E., André, ·, Ferreira De Meireles, L., Mega, F., De Figueiredo Spindler, C., Otávio, ·, Augustin, A., Gabriela, ·, Salvalaggio, S., Achaval, · Matilde, Kruse, M. S., Coirini, · Héctor, & Marcuzzo, · Simone. (2019). Severe Uncontrolled Maternal Hyperglycemia Induces Microsomia and Neurodevelopment Delay Accompanied by Apoptosis, Cellular Survival, and Neuroinflammatory Deregulation in Rat Offspring Hippocampus. *Cellular and Molecular Neurobiology*, 39, 401–414. <https://doi.org/10.1007/s10571-019-00658-8>
- Van Assche, F. A., Holemans, K., & Aerts, L. (2001). Long-term consequences for offspring of diabetes during pregnancy. *British Medical Bulletin*, 60, 173–182. <https://doi.org/10.1093/bmb/60.1.173>
- Van Lieshout, R. J., & Voruganti, L. P. (2008). Diabetes mellitus during pregnancy and increased risk of schizophrenia in offspring: A review of the evidence and putative mechanisms. *Journal of Psychiatry and Neuroscience*, 33(5), 395–404. <https://doi.org/PMID:18787655>
- Vuong, B., Odero, G., Rozbacher, S., Stevenson, M., Kereliuk, S. M., Pereira, T. J., Dolinsky, V. W., & Kauppinen, T. M. (2017). Exposure to gestational diabetes mellitus induces neuroinflammation, derangement of hippocampal neurons, and cognitive changes in

rat offspring. *Journal of Neuroinflammation*, 14(80). <https://doi.org/10.1186/s12974-017-0859-9>

Wachtmeister, L. (1998). Oscillatory Potentials in the Retina: what do they Reveal. *Progress in Retinal and Eye Research*, 17(4), 485–521. [https://doi.org/10.1016/s1350-9462\(98\)00006-8](https://doi.org/10.1016/s1350-9462(98)00006-8)

Wood, G. E., Beylin, A. V., & Shors, T. J. (2001). The contribution of adrenal and reproductive hormones to the opposing effects of stress on trace conditioning in males versus females. *Behavioral Neuroscience*, 115(1), 175–187. <https://doi.org/10.1037/0735-7044.115.1.175>

Wu, S. M., & Maple, B. R. (1998). Amino acid neurotransmitters in the retina: a functional overview. *Vision Research*, 38(10), 1371–1384. [https://doi.org/10.1016/S0042-6989\(97\)00296-4](https://doi.org/10.1016/S0042-6989(97)00296-4)

